Biogeosciences, 23, 8319–8340, 2026
https://doi.org/10.5194/bg-23-8319-2026
© Author(s) 2026. This work is distributed under
the Creative Commons Attribution 4.0 License.

Biogeosciences Open Access EGU

Fresh tephra deposits from the Tajogaite Volcano boost thermophile proliferation and soil organic matter recovery

Sara Gutiérrez-Patricio[1], Alba Gómez-Arias[1], Pedro Nolasco-Jiménez[1], Jorge Mataix-Solera[2], Javier Martínez-Martínez[3], Bruno Martínez-Haya[4], Juana Vegas[3], Nicasio T. Jiménez-Morillo[1], and Ana Z. Miller[1,5]

[1]Instituto de Recursos Naturales y Agrobiología de Sevilla(IRNAS-CSIC), Avda. Reina Mercedes 10, 41012, Seville, Spain
[2]Grupo de Edafología y Tecnologías del Medio Ambiente GETECMA, Departamento de Agroquímica y Medio Ambiente, Universidad Miguel Hernández, 03202 Elche, Alicante, Spain
[3]Instituto Geológico y Minero de España (IGME-CSIC), Rios Rosas 23, 28003 Madrid, Spain
[4]BIO-MS group, Department of Physical, Chemical and Natural Systems, Universidad Pablo de Olavide, 41013, Seville, Spain
[5]Hercules Laboratory, University of Évora, Palacio do Vimioso, 7000-809, Évora, Portugal

Correspondence: Nicasio T. Jiménez-Morillo (ntjm@irnas.csic.es) and Ana Z. Miller (anamiller@irnas.csic.es)

Received: 5 May 2025 – Discussion started: 15 May 2025
Revised: 14 October 2026 – Accepted: 4 November 2026 – Published: 13 November 2026

Abstract. Tephra fallout deposition during volcanic eruptions overlays existing soils, profoundly altering their physical, chemical, and biological properties. This study investigates the impact of the newly deposited tephra blanket from the 2021 Tajogaite eruption (La Palma Island) on the molecular composition of soil organic matter and microbial diversity across different soil horizons. To our knowledge, this is the first study combining molecular pyrolysis, stable isotope analysis, and microbial sequencing to characterize the early biogeochemical transformation of soils affected by the Tajogaite eruption. A combination of 16S rRNA gene sequencing, pyrolysis-gas chromatography/mass spectrometry (Py-GC/MS), and elemental and isotope ratio mass spectrometry (EA/IRMS) was employed. Our results reveal marked differences in organic matter composition and microbial community structure across the tephra-covered soil profile, with patterns consistent with ongoing microbial transformation of organic carbon and nitrogen compounds. The soil horizon directly beneath the tephra layer (horizon O) displayed a higher abundance of labile organic compounds and a reduced presence of recalcitrant compounds compared to the deeper horizons (A and Bw). This pattern is strongly associated with the predominance of thermophilic bacteria, which contribute actively to the breakdown of complex organic materials such as lignin and hydrocarbons, and drive key biogeochemical processes including nitrogen and carbon cycling. The continuous geothermal influence of nearby fumaroles further supports the persistence and ecological success of thermophilic communities in these volcanic soils. These findings underscore the critical role of volcanic activity not only in reshaping soil structure but also in enhancing soil fertility and resilience through microbial-mediated processes. Understanding these dynamics is essential for soil management and ecosystem recovery strategies in volcanic regions, providing new insights into the long-term effects of tephra deposition on soil health and the carbon cycle.

1 Introduction

The Tajogaite volcanic eruption, which began in September 2021 on La Palma Island (Canary Islands, Spain), was an extraordinary geological event that significantly transformed the local environment (Birnbaum et al., 2023; Troll et al., 2024). Over 85 d, the eruption released over 200 million m^3 of lava and pyroclasts, burying over 1200 ha of land and displacing 7000 residents. The voluminous ashfall, with a complex tephra blanket reaching up to 2.5 m thick, profoundly impacted the ecosystem of La Palma and posed substantial challenges for local agriculture, infrastructure, and human health (Craig et al., 2016; Bonadonna et al., 2022, 2023; Birnbaum et al., 2023; Sánchez-España et al., 2023; Biass

et al., 2024). According to these authors, the grain size of the tephra blanket varied during the eruption from lapilli (2–64 mm) to ash (< 2 mm) that spread to La Gomera, El Hierro, Tenerife and Gran Canaria islands during the more explosive phases.

Volcanic tephra is a fine-grained unconsolidated deposit, highly reactive material that can considerably modify soil structure, chemistry, and biology (Nanzyo et al., 1993; Arnalds, 2013; Wygel et al., 2019). When deposited on existing soil layers, tephra can create a new surface horizon that introduces novel mineral substrates and interacts with soil organic matter (SOM), triggering complex chemical and biological transformations (Wijesinghe et al., 2020; Peng et al., 2021). Furthermore, the interactions between volcanic ashfall and soil organic matter (SOM) can lead to the formation of polycyclic aromatic hydrocarbons (PAHs) and other condensed compounds (Nanzyo et al., 1993; Tomašek et al., 2021). These processes can influence soil fertility, stability, and overall health by modifying nutrient availability, pH, and soil aggregation (Arias et al., 2005; Peng et al., 2021; De la Rosa et al., 2023). However, these effects may be either beneficial or detrimental depending on tephra composition, deposit thickness, environmental conditions, and time since deposition. For instance, tephra may contribute to nutrient availability through mineral weathering, while thick deposits may initially limit nutrient accessibility and vegetation establishment. Additionally, volcanic ash can promote the formation of new organo-mineral complexes, altering SOM decomposition pathways and the long-term sequestration of carbon and other essential nutrients (Nierop and Buurman, 2007; Hernández et al., 2012; Iwasaki et al., 2021) to better support plant and microbial communities, ultimately influencing the trajectory of ecosystem recovery (Hernández et al., 2012; Yokobe et al., 2020; Muñoz et al., 2021). Therefore, tephra deposition can also reshape soil microbial communities by creating new ecological niches that favour specific microbial taxa adapted to volcanic substrates (Zeglin et al., 2016; Yokobe et al., 2020; Chen et al., 2021). Understanding these processes is crucial, particularly in volcanic regions where soil resilience is key to ecosystem recovery because ashfall from Tajogaite eruption has been reported to significantly impact agricultural productivity (Sánchez-España et al., 2023; Taddeucci et al., 2023). The loss of fertile topsoil and the alteration of soil properties created long-term challenges for agricultural recovery and land use (Ustiatik et al., 2023). The alteration in microbial diversity can have profound implications for soil function, influencing processes such as SOM decomposition, biogeochemical cycle of carbon and nitrogen, nutrient cycling, and the production of secondary metabolites (Gutierrez-Patricio et al., 2024).

Despite increasing interest in the ecological consequences of volcanic eruptions, the combined effects of fresh tephra deposition on SOM molecular composition and microbial community structure remain poorly understood, particularly during the early stages of soil recovery following volcanic disturbance. This study aims to characterize the molecular composition of SOM and microbial community structure within a pre-existing soil profile buried by the tephra blanket produced during the 2021 Tajogaite eruption. By integrating analytical pyrolysis (Py-GC/MS), stable isotope analysis, and 16S rRNA gene sequencing, we evaluate the interactions between newly deposited volcanic materials, organic matter transformation, and microbial colonization. Understanding these processes may provide new insights into the mechanisms driving early soil regeneration and ecosystem recovery in recently disturbed volcanic environments.

2 Material and Methods

2.1 Study site

The soil profile studied is located in the Las Manchas area of La Palma Island, within the region most affected by the 2021 Tajogaite volcanic eruption. La Palma Island, part of the Canary Islands archipelago and located approximately 400 km west of the African coast, has a total area of 708 km^2 and is one of the youngest in the archipelago, formed during the last 1.8 million years (Hoernle et al., 2009). La Palma Island shows one of the most complete records of the evolution of an oceanic volcanic island, from the Pliocene submarine basal complex, to the metamorphism originated by magmatic intrusion, the building of a Quaternary volcanic edifice, and giant landslides and intense erosion that defines the final morphology of Caldera de Taburiente (Carracedo et al., 2001; Sánchez-España et al., 2023). Volcanic activity subsequently shifted to the N–S-trending polygenetic Cumbre Nueva volcanic ridge, which has developed over the last c. 125 ka being the most active area of this island (Longpré and Felpeto, 2021).

The 2021 Tajogaite volcanic eruption, which began on 19 September and lasted for 85 d, emitted over 200 million m^3 of lava and pyroclastic materials, creating extensive lava flows that covered approximately 1200 ha and extended into the Atlantic Ocean, forming two new lava deltas (Ferrer et al., 2023). The pyroclastic materials deposited during this eruption ranged in size from fine ash to large lapilli and created a stark contrast with the pre-existing landscape (Bonadonna et al., 2022; Ferrer et al., 2023). The eruption also introduced a tephra blanket, up to 3 m thick in areas close to the volcanic cone, that overlies the native soils (Bonadonna et al., 2023).

The study site is located in the Las Manchas area (Los Llanos de Aridane municipality), situated on the western slopes of the Cumbre Nueva Ridge (Fig. 1A). Before the eruption, the soils in this area were classified as Typic Ustivitrands (Soil Survey Staff, 2022). These soils typically exhibit a sandy loam texture, low bulk density, and a high degree of aggregation, particularly in the surface horizons, which are enriched with organic matter (see Table S1).

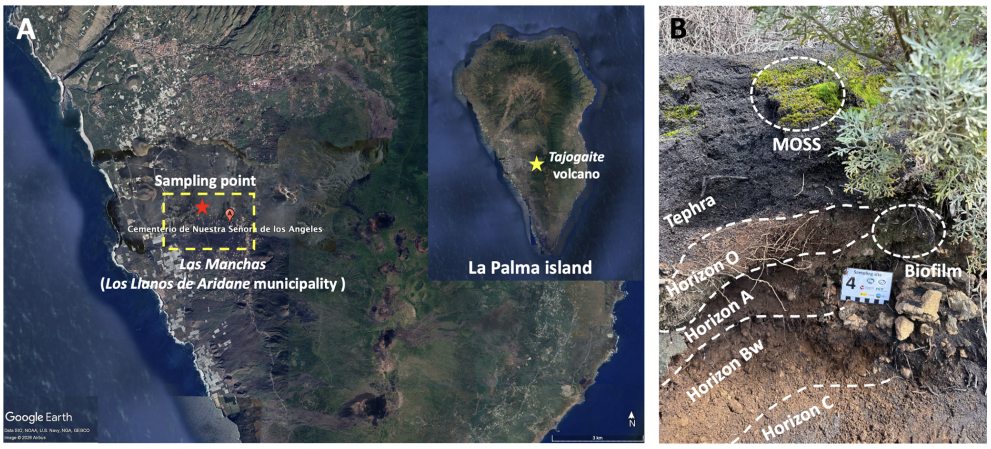


Figure 1. **(A)** Location of the soil profile beneath the tephra blanket in Las Manchas (La Palma, Spain). **(B)** Sampling area of the volcanic ash-covered soil profile, comprising moss, moss substrate (MS), biofilm located in the O horizon, and three soil horizons (O, A, and Bw). Map imagery in panel **(A)** was obtained from Google Earth (Imagery © 2026 Airbus, Map data © SIO, NOAA, U.S. Navy, NGA, and GEBCO).

Following the eruption, the pre-existing soils in the study area were buried under a 20 cm thick layer of tephra and ash. Two years after the event, mosses colonized the tephra deposit surface, and biofilms developed at the soil-tephra interface (Fig. 1B). Sampling included the collection of moss growing on the fresh tephra (MOSS), the tephra layer directly beneath the moss cover (moss substrate, MS), a dark green biofilm on horizon O (Biofilm), and three soil horizons: 0–2 cm (Horizon O), 2–10 cm (Horizon A) and 10–20 cm (Horizon Bw) (Fig. 1B). All samples analyzed in this study were composite samples, generated by collecting five subsamples per sample type across distinct sampling points and/or soil horizons, followed by thorough homogenization and pooling into a single representative mixture. This volcanic ash-derived soil profile was located near steam-emitting fumaroles, in a sector with a high temperature anomaly in the soil. These fumaroles vent water vapour as the main component and other chemical species, such as SO_2, H_2S, HCl, and CO gases up to 20.7, 17.7, > 30.0 and 19.5 ppm, respectively, at temperatures higher than the ambient (Campeny et al., 2023; Martínez-Martínez et al., 2023).

2.2 Sampling

The environmental conditions of the sampling area were monitored by installing a temperature and relative humidity sensor (HOBO MX2301A, ONSET®, Fig. S1A and B) near the fumarole vent to assess the temperature of the water vapour emissions from the fumarole. This sensor took measurements every hour for one year.

Samples were collected using sterile tools, such as spatulas or individually wrapped disposable scoops, to avoid contamination, and all samples were immediately placed into sterile Whirl-Pak bags. The samples were kept on ice during transportation to the laboratory for subsequent analysis. Subsamples of each material were used for DNA-based analysis, carbon and nitrogen elemental and isotope analysis, and molecular composition.

2.3 Carbon and nitrogen elemental and isotope analysis

The compositional analysis of organic carbon and nitrogen in both pyroclastic materials and soil samples was carried out using a (EA/TCD; Thermo Scientific in Bremen, Germany). Samples, ranging in weight from 5 to 10 mg, were processed in duplicate ($n = 2$) following a decarbonization treatment as outlined by Jiménez-Morillo et al. (2016a, 2020a). Briefly, samples were treated with 10 % HCl for 24 h to eliminate carbonate phases and subsequently rinsed with deionized water until a neutral pH was reached. The treated samples were then dried at 65 °C before isotopic analysis. The calibration of carbon and nitrogen content employed certified standards such as acetanilide, nicotinamide, and aspartic acid, provided by Thermo Scientific, Bremen, Germany. The carbon and nitrogen isotope ratios ($^{13}C/^{12}C$ and $^{15}N/^{14}N$) were determined using an Elemental Analyzer connected to a Thermo Fisher Delta V Advantage Isotope Ratio Mass Spectrometer (EA/IRMS), following the method described by (Jiménez-Morillo et al., 2020b). These procedures were conducted at the Stable Isotope Laboratory – MOSS at IRNAS-CSIC (Spain). Isotope values are expressed in delta (δ) notation in parts per thousand (‰) relative to certified standards set by the International Atomic Energy Agency (IAEA). For $\delta^{13}C$, the standards were: cellulose (IAEA-CH-3, $\delta^{13}C = -24.7$ ‰); sucrose (IAEA-CH-6, $\delta^{13}C = -10.5$ ‰), and caffeine (IAEA-600, $\delta^{13}C = -27.8$ ‰), while for $\delta^{15}N$, the standards were: caffeine (IAEA-600, $\delta^{15}N = 1.0$ ‰); ammonium sulfate (IAEA-N1, $\delta^{15}N = 0.4$ ‰), and ammonium sulfate (IAEA-N2, $\delta^{15}N = 20.4$ ‰) with a standard deviation

for bulk $\delta^{13}C$ of ± 0.05 ‰ and $\delta^{15}N$ of ± 0.1 ‰. Two subsamples ($n = 2$) of both the samples and the standards were analysed by EA/IRMS, and each subsample was analysed in duplicate as technical replicates.

2.4 Analytical pyrolysis (Py-GC/MS)

The analytical pyrolysis (Py-GC/MS) technique was composed of (i) a double-shot pyrolyzer, model 3030D (Frontier Laboratories, Japan), set at 500 °C; (ii) an Agilent 6890N gas chromatograph, and (iii) an Agilent 5973 MSD (mass selective detector) mass spectrometer, operating at an electron impact energy of 70 eV. The chromatographic separation involved an HP-5MS UI capillary column (30 m length, 0.25 mm internal diameter, 0.25 µm film thickness) with a helium flow rate of 1 mL min^{-1}. The sample injection was conducted in splitless mode at 250 °C, and the temperature program was adopted from protocols described by Jiménez-Morillo et al. (2020a). Ion fragments ranging from 50 to 550 m/z were recorded, and compound identification was conducted by comparison with virtual spectral libraries, such as the NIST20 and Wiley7. The molecular compounds released by Py-GC/MS were categorized into the eight biogenic families proposed by Jiménez-Morillo et al (2016a): unspecific aromatic compounds (ARO), polysaccharides (POL), peptides (PEP), lignin (LIG), lipids (LIP), nitrogen-containing compounds (N-comp), polycyclic aromatic hydrocarbons (PAHs), and steranes (STR). Chromatographic peak area > 0.2 % of the total chromatographic area was not taken into account. For a detailed study of homologous series of n-alkanes and n-alken-2-ones, single ion monitoring of specific fragments – specifically ions with m/z 57 and m/z 59, respectively – was adopted.

2.5 DNA extraction and 16S rRNA gene amplicon sequencing

Genomic DNA was extracted from 250 mg of each sample ($n = 6$) using the DNeasy PowerSoil Pro Kit (Qiagen, Germany) following the manufacturer's instructions. DNA concentration was quantified using a Qubit 4.0 fluorometer (Invitrogen).

The V3–V4 hypervariable region of the prokaryotic 16S rRNA gene was amplified using the universal primers 341F (5′-CCTACGGGNGGCWGCAG-3′) and 805R (5′-GACTACHVGGGTATCTAATCC-3′) with Illumina overhang adapter sequences, following Klindworth et al. (2013). Amplicon libraries were sequenced on an Illumina MiSeq platform using 2×250 bp paired-end chemistry. Library preparation and sequencing were performed by Novogene Sequencing Services (China).

Raw sequencing reads were deposited in the NCBI Sequence Read Archive (SRA) under accession PRJNA1192049.

2.6 Bioinformatic processing

Raw paired-end reads were processed using QIIME 2 (v2024.5) (Bolyen et al., 2019). Primer sequences were removed prior to denoising to prevent primer-derived artifacts and to improve read merging. Reads were then quality filtered and denoised using the q2-dada2 plugin (Callahan et al., 2016), which infers exact amplicon sequence variants (ASVs) by modeling sequencing errors and resolving unique biological sequences. Forward and reverse reads were merged to reconstruct the full V3–V4 amplicon, generating an ASV feature table for downstream ecological analyses. Chimeric sequences produced during PCR amplification were identified and removed using the consensus approach implemented in DADA2, reducing spurious diversity. Taxonomy was assigned with a Naïve Bayes classifier trained on the V3–V4 region against the SILVA reference database (release 138) (Quast et al., 2013), ensuring that taxonomic classification was optimized for the targeted amplicon region.

2.7 Diversity and statistical analyses

All analytical measurements were performed in duplicate, and results are reported as mean values with their corresponding standard deviations. Statistical differences among samples were evaluated using one-way analysis of variance (ANOVA) followed by Tukey's post hoc test at a significance level of $p < 0.05$. These analyses were used to identify statistically significant differences in elemental and isotopic composition among the different soil horizons, biofilm samples, and moss substrates. Correlation analyses between $\delta^{13}C$ and carbon content were performed using linear regression in order to evaluate relationships between isotopic composition and organic carbon abundance.

Alpha diversity analyse was computed in QIIME 2 (v2024.5). Alpha diversity was calculated to summarize within-sample diversity using richness and diversity indices (e.g., observed ASVs, Chao1, Shannon, and Simpson, as appropriate). To aid interpretation of the ordination, we produced a PCoA biplot by projecting (i) geochemical/pyrolytic descriptors (e.g., compound-class abundances from pyrolysis and elemental contents) and (ii) the relative abundances of dominant microbial phyla onto the same ordination space. Vectors (arrows) represent the direction of increasing values for each variable and their strength of association with the ordination axes (longer vectors indicate stronger relationships). This combined representation was used to highlight which chemical pools and microbial groups co-varied across samples and to identify the main gradients driving separation along PCo1 and PCo2.

3 Results and discussion

3.1 Elemental and isotope composition of carbon and nitrogen

Table 1 depicts the average values and standard deviations of the elemental and isotope composition of total organic carbon (TOC) and nitrogen (N) in Moss, moss substrate (MS), Biofilm, and three soil horizons (Horizon O, A, and Bw). Horizon O samples exhibited the highest average of TOC (between 1.4 and 6.4-fold), which may be associated with a noticeable root layer (Fig. 1). The content of N was also the highest, although no significant difference was found with the Biofilm sample collected from Horizon O. The Biofilm also shows notable TOC, and its ratio TOC/N close to 9 (8.83 on average) indicates that the biofilm was found in a healthy state. Previous studies have shown that biofilms with C/N ratio close to 9 have higher concentrations of carbohydrates and proteins in the biofilm and a significant upregulation of the Quorum Sensing genes (Ramos et al., 2023).

In contrast, the TOC and N values in the Horizons A (17.6±3.39 and 1.6±0.51, respectively) and Bw (8.65±4.48 and 0.95 ± 0.87, respectively) were consistent with those reported in different soil types. The concentration of both elements in Horizon A is three-fold of those found in B, indicating a decline in TOC and N content with increasing soil depth (Girona-García et al., 2018; Jiménez-Morillo et al., 2020a). For Moss and moss substrate (MS), the higher TOC content in MS compared to Moss could be attributed to the presence of numerous small moss roots, which form a three-dimensional network that aggregates and stabilizes lapilli grains. Additionally, the presence of root exudates, rich in C and N compounds, may contribute to this remarkable concentration of organic compounds (Sokolova, 2020). The observed moss colonization is consistent with the patterns described in previous studies of volcanic environments, which highlight the role of mosses and other photosynthetic organismsas pioneer colonizers during the early stages of ecosystem development (Smith, 1984; Ingimundardóttir et al., 2014; Vilmundardóttir et al., 2018; Dragone et al., 2023).

Regarding the C isotope composition, all samples exhibited δ^{13}C values within the typical range for C_3 plants (between −25 ‰ and −35 ‰ (Katsumi et al., 2015; Ghezzi et al., 2024). However, significant differences were observed among the samples. Moss, Horizon O, and Biofilm displayed the most negative δ^{13}C values (−28.5 ‰ ± 0.1, −28.4 ‰ ± 3.5, and −29.2 ‰ ± 1.6, respectively), which reflected the presence of fresh organic matter (Jiménez-Morillo et al., 2020b). In contrast, samples from the A and Bw soil horizons and the moss substrate (MS) were enriched in ^{13}C (Table 1). This trend has also been observed by Girona-García et al. (2018) in soil profiles under pine and beech forests, where deeper horizons exhibited higher δ^{13}C values. Such ^{13}C-enrichment in soil samples is often associated with more humified organic matter (Jiménez-Morillo et al., 2020b). The

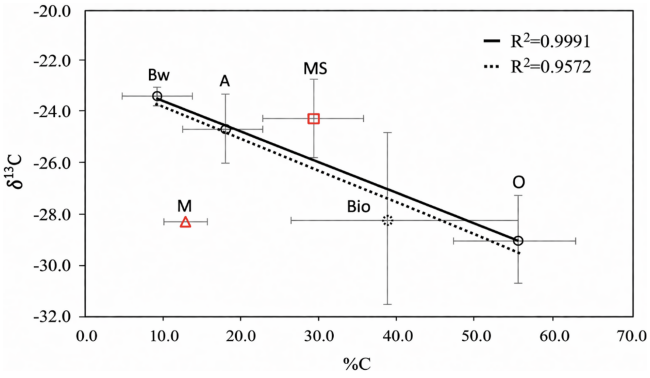


Figure 2. Plot of average ($n = 2$) δ^{13}C (‰, V-PDB) vs. % C of Moss (red triangle), moss substrate (MS, red square), Biofilms (black dashed circle) and soil horizons O, A and Bw (open black circles) with linear regression of horizons (solid line) and including biofilms (dashed line).

observed ^{13}C-enrichment of the MS (about 4 ‰–5 ‰ above Moss, Biofilm and Horizon O samples), may be attributed to (i) the heavier isotope signature of root exudates compared to other organic compounds commonly found in soil samples (Girona-García et al., 2018), and (ii) microbial activity linked to diverse families of microorganisms (Jiménez-Morillo et al., 2020b; Miller et al., 2022; San-Emeterio et al., 2023). In addition, Horizons A and Bw have similar δ^{13}C values (−24.8±1.3 and −23.5±0.4, respectively) to the MS, which is mainly composed of tephra. This could be indicative of the volcanic origins of the paleo soil (Horizons A and B) (Carracedo et al., 2022) and suggests that the recurrent tephra deposition, and consequently burying of soil, after each volcanic eruption may have affected the carbon cycle during the soil formation (Matus et al., 2014 and references therein).

There is a strong negative correlation observed between δ^{13}C values and TOC content across the different soil horizons and the Biofilm (Fig. 2). This trend is particularly pronounced in the soil horizon samples ($R^2 = 0.9991$; solid line). However, when the biofilm (Bio, Fig. 2) sample is included, the correlation weakens slightly ($R^2 = 0.9572$; dashed line).

This negative correlation between δ^{13}C and TOC content has been previously described in soils worldwide. In all cases, this trend has been attributed to either the decomposition of organic matter, the fractionation by microbial activity or the shift of a predominant contribution from plants to microorganisms in the residual organic matter as it progresses through the soil horizons (Ågren et al., 1996; Volk et al., 2018; Ehleringer et al., 2000; Krüger et al., 2024). The microbial activity may process fresh organic matter, leaving behind evolved (humified) material with a heavier isotope. This alteration may also reduce the TOC content due to microbial respiration. A similar pattern has been observed in the isotope composition of highly humified (evolved) organic matter associated with very fine sand particles in shal-

Table 1. Isotope and elemental composition of nitrogen (N) and total organic carbon (TOC) of Moss, moss substrate (MS), Biofilm and three soil horizons (O, A and Bw). Different letters denote significant differences between samples (one-way ANOVA with Tukey's HSD post-hoc test, $\alpha = 0.05$).

Sample	δ^{15}N (‰, V-Air)	δ^{13}C (‰, VPDB)	N (%)	TOC (%)
Moss	-5.1 ± 0.4d	-28.5 ± 0.1b	0.62 ± 0.12b	12.53 ± 1.69c
MS*	5.0 ± 2.9bc	-24.3 ± 1.6ab	3.17 ± 0.80ab	28.71 ± 4.53bc
Biofilm	1.9 ± 0.9c	-28.4 ± 3.5ab	4.37 ± 1.86a	38.59 ± 16.65ab
Horizon O	7.9 ± 0.5b	-29.2 ± 1.6b	4.99 ± 0.78a	55.27 ± 8.09a
Horizon A	6.0 ± 0.4bc	-24.8 ± 1.3ab	1.60 ± 0.51b	17.60 ± 3.39bc
Horizon Bw	16.6 ± 3.1a	-23.5 ± 0.4a	0.95 ± 0.87b	8.65 ± 4.48c

* MS = moss substrate

low soil layer (Jiménez-Morillo et al., 2020a), which may confirm the influence of microorganisms in the humification process of fresh organic matter. However, the ratio between δ^{13}C and TOC for Moss and the tephra collected under the moss (MS) did not correlate with the soil. This is probably because the samples were collected shortly after the volcanic eruption that accumulated the tephra over the previous soil (Horizon O). Indicating that the C cycle of the tephra layer was still in an early stage of the andisol formation process, preventing the observation of statistical correlations between the soil samples and the tephra. Future analyses of the same tephra layer could better constrain the process of andisol formation as it gets closer to the regression line of horizons depicted in Fig. 2.

Regarding the nitrogen isotope composition (δ^{15}N), the Moss sample showed the lowest δ^{15}N value (Table 1), a typical characteristic for mosses (Zechmeister et al., 2008). In contrast, the other samples displayed positive δ^{15}N values (Table 1). For the MS sample, the ^{15}N-enrichment and their statistical similarity with δ^{15}N values observed in the soil and biofilm samples suggest that it could be derived from the activity of certain microorganisms, such as cyanobacteria, that utilize nitrogen-derived compounds excreted by the moss roots (Carrell et al., 2022). In addition, the deepest soil sample (Horizon Bw) showed the highest δ^{15}N enrichment, which could be associated with denitrification processes (Girona-García et al., 2018). While humification is well known to cause ^{15}N-enrichment, particularly in forest soils (Szpak, 2014), ^{15}N-depletion can occur during the uptake of inorganic N by vegetation (Högberg, 1997). Therefore, the observed trend can be best explained by the alteration of biomass by heterotrophic organisms, which produce ^{15}N-depleted compounds while progressively enriching the remaining biomass with ^{15}N over time (Billings and Richter, 2006; Makarov, 2009; Szpak, 2014; Girona-García et al., 2018).

3.2 Molecular composition of organic fraction

The use of analytical pyrolysis (Py-GC/MS) has revealed remarkable molecular differences between soil, moss substrate (tephra), Biofilm, and Moss samples (Fig. 3). The Moss sample is rich in organic compounds, particularly lipids (31.56 %) and polysaccharides (29.75 %), aligning with findings from previous studies (Klavina et al., 2015; Petkova et al., 2023). Among the lipid compounds identified were essential oils, such as α-Terpinene and Phytol, n-alkanes (e.g., heptadecane, heneicosane; Klegin et al., 2023) and n-alkanoic acids (e.g., 9,12,15-Octadecatrienoic acid, 13-Eicosenoic acid, 22-Tricosenoic acid; Yucel, 2021; Klegin et al., 2023). Polysaccharides are commonly associated with bryophytes such as mosses, serving as structural components and also assumed to contribute to stress tolerance (Klavina et al., 2015). In this study, the identified polysaccharides were primarily furans (e.g., 2(5H)-Furanone, 5-methyl-, 2-Furancarboxylic acid, methyl ester, 3-Furaldehyde) and levoglucosan (β-D-Glucopyranose, 1,6-anpah). However, due to dehydration and molecular restructuring during pyrolysis, complete identification of polysaccharides is not feasible, and other polysaccharides may be present (González-Pérez et al., 2016). The molecular analysis also revealed a significant presence of non-specific aromatic compounds (13.60 %) and peptide compounds (11.69 %). Among the aromatic compounds, phenol derivatives such as Phenol, 2-methyl-, Phenol, 2,3-dimethyl-, 1,2-Benzenediol, and Phenol, 2,3,5-trimethyl were prominent. These phenolic compounds are considered critical in early plant evolution, particularly in moss growth and cuticle permeability, which were key for adaptation to terrestrial environments (Renault et al., 2017). Such phenolic compounds are precursors to lignin, synthesized by the phenylpropanoid pathway, which strengthens cell walls, aids in water transport, and supports upright growth (Fraser and Chapple, 2011). Peptide-derived compounds were also found, with their primary function being the defence of mosses against environmental stressors such as drought and high temperatures (Ren et al., 2024). Additionally, these peptides provide resistance against micro-

bial pathogens (Valeeva et al., 2022). Plants produce a range of bioactive metabolites, peptides, and small molecules that contribute to defence mechanisms and microbial resistance (Valeeva et al., 2022), which may explain the presence of some of the compounds detected in the Moss sample. In addition, peptide compounds are crucial regulators of ecosystem function because they can provide direct nutrient supplies to soil microorganisms and plants (Wang et al., 2023).

Only a few organic compounds were identified in the MS samples, mainly high molecular weight alkyl lipids (*n*-alkanes) and sterols, being the latter the dominant group (65 %). Key sterols detected include Stigmastan-3,5-dien, Campesterol, and γ-Sitosterol, also found in the Moss sample (Table S2). The presence of Campesterol and γ-Sitosterol may indicate an input of organic matter from the moss via rhizoid exudates. Sterols are crucial for various plant physiological processes, not only supporting cell membrane structure and fluidity but also acting as hormone precursors and playing a role in responses to biotic and abiotic stress (Valitova et al., 2016; Cabianca et al., 2021). In addition, the presence of high molecular weight alkyl compounds, originating from epicuticular waxes, supports the hypothesis that there is a direct input of organic material from the moss to the substrate (tephra). The δ^{13}C value observed in this sample does not align with the molecular composition identified by Py-GC/MS, as the detected compounds usually exhibit a markedly negative isotope signature (Park and Epstein, 1961; San-Emeterio et al., 2023). However, the observed ^{13}C-enrichment in this sample against the moss could be attributed to low-molecular-weight polysaccharide-derived compounds undetected by this analytical technique.

The Biofilm sample collected from Horizon O consists mainly of lipids (40.54 %), non-specific aromatic compounds (38.36 %), polysaccharides in the form of furans (13.08 %), and peptides (8.02 %). This molecular composition aligns perfectly with the main molecular composition found in Biofilm samples analyzed in different volcanic regions (Miller et al., 2020; Ghezzi et al., 2024; Palma et al., 2024). The lipid composition is mainly dominated by *n*-alkane/alkene pairs with different proportions, which will be discussed in the Sect. 3.3.1.

The Horizon O sample is dominated by lipid compounds (42.43 %), mainly alkyl compounds (*n*-alkane/alkene pairs and *n*-alkanoic acids), followed by aromatic moieties (17.80 %) and polysaccharides (12.57 %). In addition, this is the only sample with a relatively high concentration of methoxyphenols, i.e., lignin-derived compounds (12.18 %). The abundance of alkyl compounds suggests the existence of different organic fractions from distinct origins: (i) organic matter from pre-eruption vegetation, also indicated by the δ^{13}C of the Horizon O sample (-29.2 ± 1.6) typical of C_3 plants, (ii) the degradation of lipid membranes from microorganisms induced by the deposition of tephra during the Tajogaite volcanic eruption, and (iii) highly evolved organic matter from post-eruption microbial activity in the soil (Jiménez-Morillo et al., 2017; Bull et al., 2000; Jiménez-Morillo et al., 2016b; Leal et al., 2023). In contrast, the presence of lignin- and polysaccharide-derived compounds probably indicates the recent input of herbaceous/shrubby plant material (Fig. 1). It could also stem from root exudates of vegetation present before the ash deposition, supported by the high concentration of roots in the Horizon O (Fig. 1). Lignin compounds, particularly from the guaiacol and syringol groups, confirm a contribution of tree-derived organic matter (San-Emeterio et al., 2023). However, the greater abundance of guaiacol over syringol suggests ongoing microbial degradation activity, as syringol is more easily degraded by microorganisms (San-Emeterio et al., 2023). Additionally, condensed compounds (PAHs) were found in the shallow horizon. This could be generated by: (i) ancient fires with particles trapped in the soil layers (Jiménez-Morillo et al., 2016b), (ii) high-temperature vapour emissions, from volcanic fracture, leading to defunctionalization and condensation of polar aromatic compounds (Capaccioni et al., 1995) or, (iii) microbial activity. Several pathways have been described for hydrocarbon synthesis by microorganisms (Ladygyna et al., 2006 and references therein). Some of these biogenic PAHs have been detected in forest soil (Krauss et al., 2005) with high degradation of lignin, in peatlands and wetlands (Wakeham and Canuel, 2016), where organic matter accumulates and transforms slowly, and in lake and marine sediments (Love et al., 2021), where microbial activity and anoxic conditions promote the polymerization of aromatic compounds.

The two deepest Horizons (A and Bw) of the soil profile share a similar molecular composition, dominated by non-specific aromatic compounds, lipid compounds (mainly *n*-alkane/alkene pairs), polysaccharides and peptides, with a complete absence of lignin molecules. This pattern has been observed in forest soils across the Iberian Peninsula (Aznar et al., 2016; Jiménez-Morillo et al., 2016a; De la Rosa et al., 2019), indicating the presence of microbial-derived compounds and linked to high microbial activity (Jiménez-Morillo et al., 2018). The abundance of non-specific aromatic compounds may also result from fungal degradation of plant lignins (Kellner et al., 2014). However, important differences include a higher proportion of condensed compounds (PAH = 15.17 %) in the upper Horizon, while the deeper Horizon has more sterane compounds (10.76 %). In the Horizon A, highly condensed PAHs, such as phenanthrene and pyrene suggest the presence of pyrogenic material, usually associated to organic matter combustion (González-Pérez et al., 2014; Miller et al., 2020, 2022). In contrast, the deeper Horizon only contains branched naphthalene compounds, possibly due to lower-intensity fires or microbial degradation of condensed compounds by thermophiles (Musat et al., 2009; Mohapatra and Phale, 2021). In the sterane family, the deeper Horizon (Bw) contains Stigmastan-3,5,22-triene, Ergosta-4,6,22-trien-3-ol, and Friedelan-3-one. These plant- and fungi-synthesized compounds are well-preserved in deeper layers due to their stability (Kristan and Rižner,

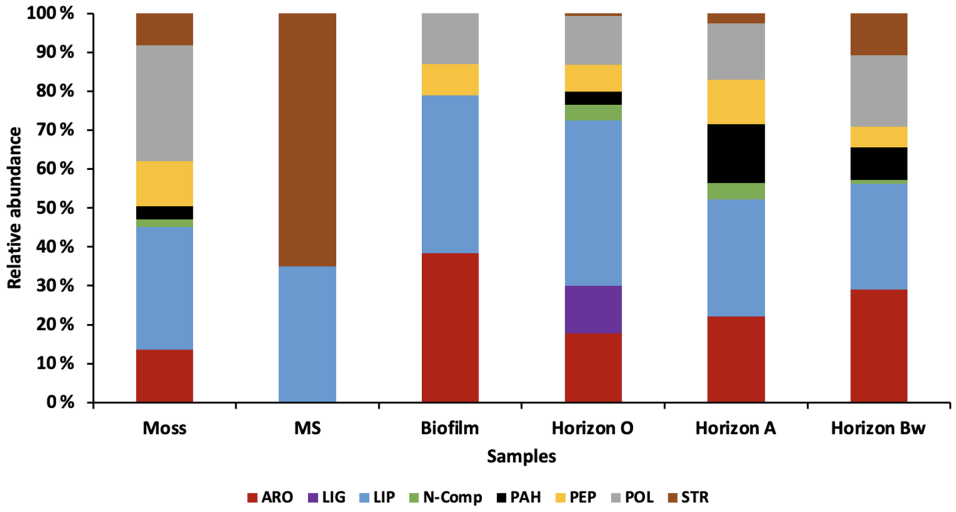


Figure 3. Relative abundance (%) of the main organic families identified by Py/GC/MS from Moss, moss substrate (MS), Biofilm, and soil horizons (O, A, Bw) samples. The main organic families are: unspecific aromatic compounds (ARO), polysaccharides (POL), peptides (PEP), lignin (LIG), lipids (LIP), nitrogen-containing compounds (N-comp), polycyclic aromatic hydrocarbons (PAHs), and steranes (STR).

2012), with clear accumulation in the lower horizons, while they are almost absent in the Horizon O and the B (Fig. 3).

3.3 Lipid analysis by Py-GC/MS

3.3.1 *n*-Alkanes

The *n*-alkane series were identified using m/z 57 in the selected-ion-monitoring (SIM) chromatogram (Fig. 4). Chain lengths ranged from C_{10} to C_{35}, reflecting various organic matter sources (Jiménez-Morillo et al., 2017). In the Moss sample, a bimodal distribution was observed with peaks at *n*-pentadecane (C_{15}) and *n*-hentriacontane (C_{31}), with odd-chain *n*-alkanes predominating, especially in longer chains ($> C_{25}$). This suggests *n*-alkanes from moss epicuticular waxes, with a peak at *n*-hentriacontane (Schwark et al., 2002). The presence of low-molecular-weight (LMW) *n*-alkanes ($< C_{20}$) may point to associated microorganisms, as LMW *n*-alkanes typically originate from microbial cell walls (Jiménez-Morillo et al., 2017, 2022).

In the MS sample, the dominance of odd-chain high-molecular-weight (HMW) *n*-alkanes supported direct organic matter input from moss. However, the abundance of *n*-tritriacontane (C_{33}) and *n*-pentatriacontane (C_{35}) *n*-alkanes may also indicate C4 vegetation (Vogts et al., 2009; Feakins et al., 2016) or the adaptation of pre-eruption vegetation to water stress caused by volcanic ash.

In Horizon O, a bimodal *n*-alkane distribution with peaks at C_{15} and *n*-docosane (C_{22}) suggested the presence of organic matter from soil microorganisms or the degradation of plant biomass by microorganisms over time (Jiménez-Morillo et al., 2016b, 2017). The gradual decline in HMW *n*-alkanes and the absence of a clear odd-over-even pattern indicates microbial degradation processing of organic matter (de Blas et al., 2013; Jiménez-Morillo et al., 2022; Leal et al., 2023). The higher root density in this layer could also contribute to the observed *n*-alkane pattern.

The Biofilm sample was dominated by LMW *n*-alkanes, confirming its microbial origin (Jiménez-Morillo et al., 2017). The presence of branched alkanes like neophytadiene, 2,6,10-trimethyltridecane, and 2,6,11-trimethyldodecane further supports a microbial contribution (Palma et al., 2024).

In deeper horizons (A and Bw), there is a clearer differentiation between LMW and HMW *n*-alkanes, indicating two carbon pools from microorganisms (LMW *n*-alkanes) and plant vegetation biomass (HMW *n*-alkanes). The microbial fraction may stem from lipidic membranes (Miller et al., 2016) or microbial degradation of plant biomass, such as alkyl compounds from lignocellulose breakdown (Rabbi et al., 2014; Jiménez-Morillo et al., 2022; Miller et al., 2022). The nonspecific aromatic compounds previously discussed also suggest the lignin breakdown process. However, the most significant differences among horizons are seen in HMW *n*-alkanes. The Horizon A peaks at *n*-nonacosane (C_{29}), indicating tree or shrub vegetation, while the Horizon Bw peaks at *n*-hentriacontane (C_{31}), suggesting herbaceous vegetation (Bull et al., 2000). Therefore, results indicate a change in vegetation probably due to the alteration of the environmental conditions.

3.3.2 *n*-Alkane-2-ones

The pyrolyzed samples from La Palma, except for the Biofilm sample, revealed a series of *n*-alkane-2-ones (m/z 59 ion chromatograms) ranging from C_{17} to C_{31}, with a general odd-over-even chain-length predominance (Fig. 5). However, each sample showed distinct patterns. In the Moss sample, the maximum was at *n*-alkane-2-one C_{23}, without a clear

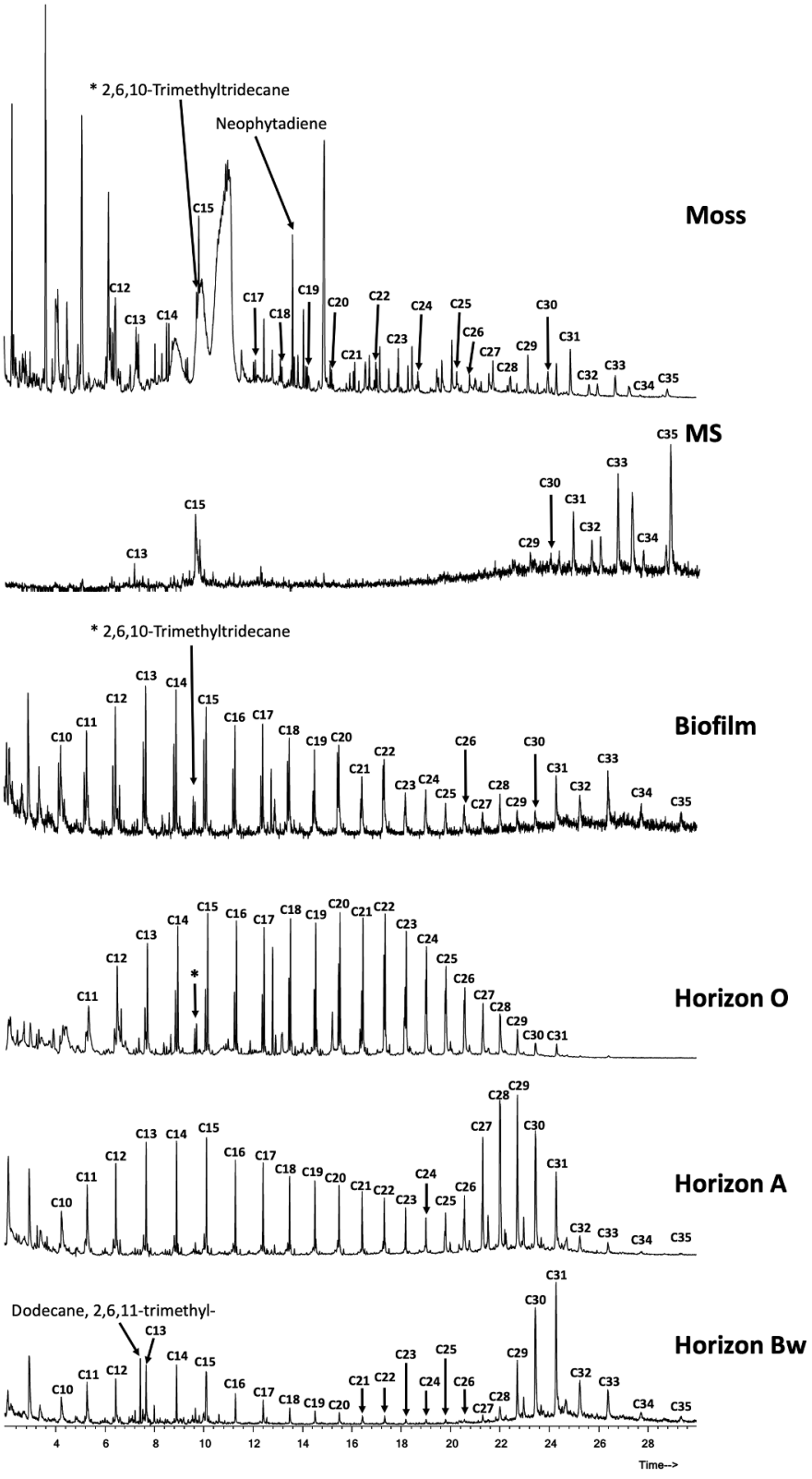


Figure 4. *n*-alkane (m/z 57) distribution obtained by direct pyrolysis (Py-GC/MS) of Moss, moss substrate (MS), Biofilms and soil horizons (O, A and Bw) samples.

parity pattern, though the odd-over-even trend was evident in LMW *n*-alkane-2-ones. This suggests a mixture of lipids from both the moss and its associated microbiome, as also seen in the *n*-alkanes (Fig. 4).

The MS sample showed a *n*-alkane-2-ones distribution similar to that observed for *n*-alkanes (Fig. 4), being dominated by C_{27} and C_{31} molecules, which supports the idea of a direct contribution of organic matter from the Moss.

The soil horizons showed differences in the *n*-alkane-2-one distribution (Fig. 5). In Horizon O, the maximum was at *n*-alkane-2-one C_{21}, while in horizons A and Bw, the maxima were at C_{25} and C_{27}, respectively. The Horizon O had a range of *n*-alkane-2-ones from C_{17} to C_{29}, suggesting more degraded organic matter, possibly due to fine ash deposition affecting organic matter or microorganisms. In Horizon A, the *n*-alkane-2-one distribution resembled typical soils, with two carbon pools: (i) LMW *n*-alkane-2-ones from microbial activity, and (ii) HMW ones from plant-derived organic matter (Jaffé et al., 1996; Kumar et al., 2020). This aligns with the *n*-alkane distribution (Fig. 4) and overall molecular analysis (Fig. 3). In contrast, the Horizon Bw contained only HMW *n*-alkane-2-ones ($> C_{25}$), considered biomarkers of vegetation (Kumar et al., 2020; Palma et al., 2024). This aligns with the isotope carbon signature observed in the soil (Table 1 and Fig. 2) that indicates the influence of microbial processes at the top layer (Horizon O) and a gradual shift to plant-influenced processes towards the bottom (Horizon Bw). The absence of LMW *n*-alkane-2-ones in Horizon Bw could be due to concentrations below detection limits, as this horizon had low TOC (Fig. 1). Environmental factors such as moisture and nutrient availability may affect *n*-alkane-2-one formation by altering the degradation of *n*-alkanes and *n*-alkanoic acids (Lehtonen and Ketola, 1990; Zhang et al., 2004). Zhang et al. (2004) identified potential sources of *n*-alkane-2-ones, including: (i) epicuticular waxes from plants; (ii) microbial oxidation of *n*-alkanes; (iii) β-oxidation and decarboxylation of *n*-alkanoic acids; and (iv) microbial cracking of HMW *n*-alkane-2-ones into LMW ones. The predominance of LMW *n*-alkane-2-ones in Horizon O further supports an active microbial contribution to organic matter transformation.

3.4 Bacterial community composition

A total of 198.129 ASVs (amplicon sequence variants) were analysed from 16S rRNA gene sequencing. The richness and evenness of microbial communities were estimated using Chao1, Shannon and Simpson indices (Table 2). The Biofilm was the most biodiverse sample, with the highest species richness, and Shannon and Simpson indices of 7.860 and 0.989, respectively, followed by horizons Bw and A and Moss. In contrast, Horizon O showed a lower diversity, with Shannon and Simpson indices of 4.166 and 0.689, respectively. According to the Chao1 richness estimator, Horizon O and the Biofilm showed the highest predicted microbial richness. The close agreement between the Chao1 estimates and observed richness in both Horizon O and the Biofilm suggests that the sequencing effort captured most of the estimated microbial richness, with only a small proportion remaining undetected.. It is noteworthy that the microbial community in the tephra collected beneath the moss (MS) reached a substantial diversity and richness within just two years following the deposition of the Tajogaite volcanic tephra, because it suggests a rapid microbial colonization of the volcanic substrate.

Table 2. Alpha diversity 16S of Moss, moss substrate (MS), Biofilms and soil horizons samples.

Sample	Shannon	Simpson	Chao1	Observed
Moss	6.359	0.973	426.143	426
MS	5.522	0.950	255.500	254
Biofilm	7.860	0.989	832.783	832
Horizon O	4.166	0.689	833.948	829
Horizon A	6.531	0.972	510.315	473
Horizon Bw	7.321	0.972	814.125	812

Most of the sequences identified belong to the Bacteria kingdom; however, Archaea, was also found, primarily in the Moss, Biofilm and MS samples, comprising 2.63 %, 2.48 % and 1.31 %, respectively (Fig. 6A). They have been reported as early colonizers in samples from the volcanic island Hunga Tonga Hunga Ha'apai, in the Kingdom of Tonga (Fujimura et al., 2016; Dragone et al., 2023). Archaea are known for their ability to inhabit extreme environments and play critical roles in biogeochemical cycles (Offre et al., 2013; Martínez-Espinosa, 2020). The main archaeal class detected in these samples was *Nitrososphaeria*, belonging to the phylum *Nitrososphaerota*, which plays a key role in the nitrogen cycle by transforming ammonia into nitrite, thereby contributing to the nitrogen availability in the soil. This process indirectly supports plant nutrition (Leininger et al., 2006; Lehtovirta-Morley et al., 2024) and influences the distribution of N concentration described in the Biofilm and MS samples. The presence of N in these samples infers that the identified class *Nitrososphaeria* is oxidizing the ammonium to nitrite, which requires the presence of oxygen. This might explain the presence of these archaea only in the Moss, MS and Biofilm samples, which are in contact with the atmosphere.

The bacterial phylum *Pseudomonadota* was found in all samples, with relative abundances decreasing with depth, ranging from 58.1 % (Moss) to 5.6 % (Horizon Bw). Members of this phylum included *Acidibacter, the Craurococcus-Caldovatus* bacteria group, and the *Methyloligellaceae* family (Fig. 6B). The acidophilic, ferric iron-reducing, heterotrophic bacterium *Acidibacter*, previously isolated from the Guadiana pit lake, currently has only one described species (Falagán and Johnson, 2014). This bacterium was

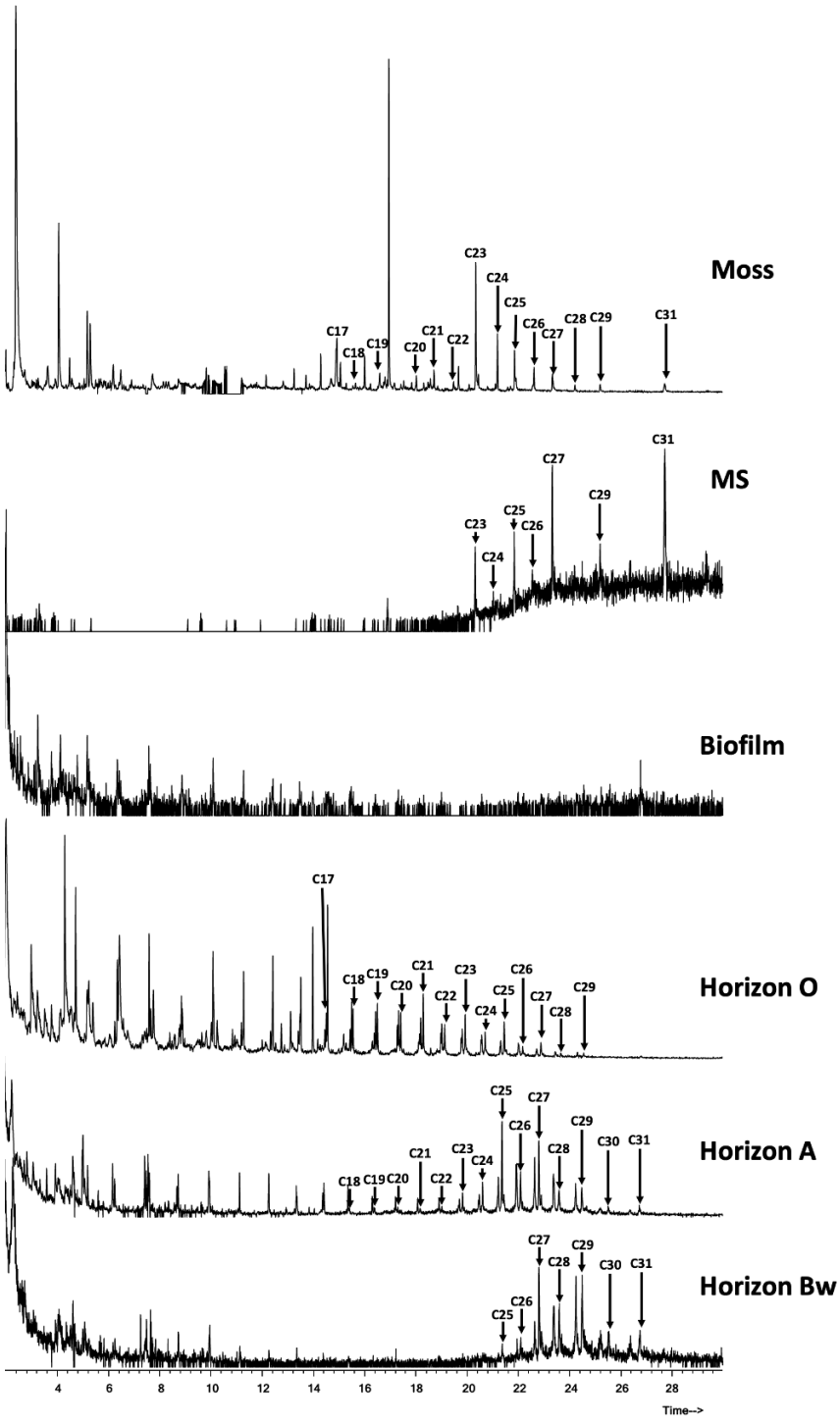


Figure 5. *n*-alkan-2-one (m/z 59) distribution was obtained by direct pyrolysis (Py-GC/MS) of Moss, moss substrate (MS), Biofilms and soil horizons (O, A and Bw) samples.

found in all three horizons, although its abundance decreased with depth, indicating its adaptation to metabolize fresh organic matter, which is more abundant in the Horizon O. The *Caldovatus* genus, a thermophilic bacterium, was found in the MS sample (6.29 %). This genus includes only two described species, *C. aquaticus* and *C. sediminis* (Habib et al., 2017; Hu et al., 2022). The *Methyloligellaceae* family is characterised by its ability to use methane as a carbon and energy source, playing a key role in the carbon cycle

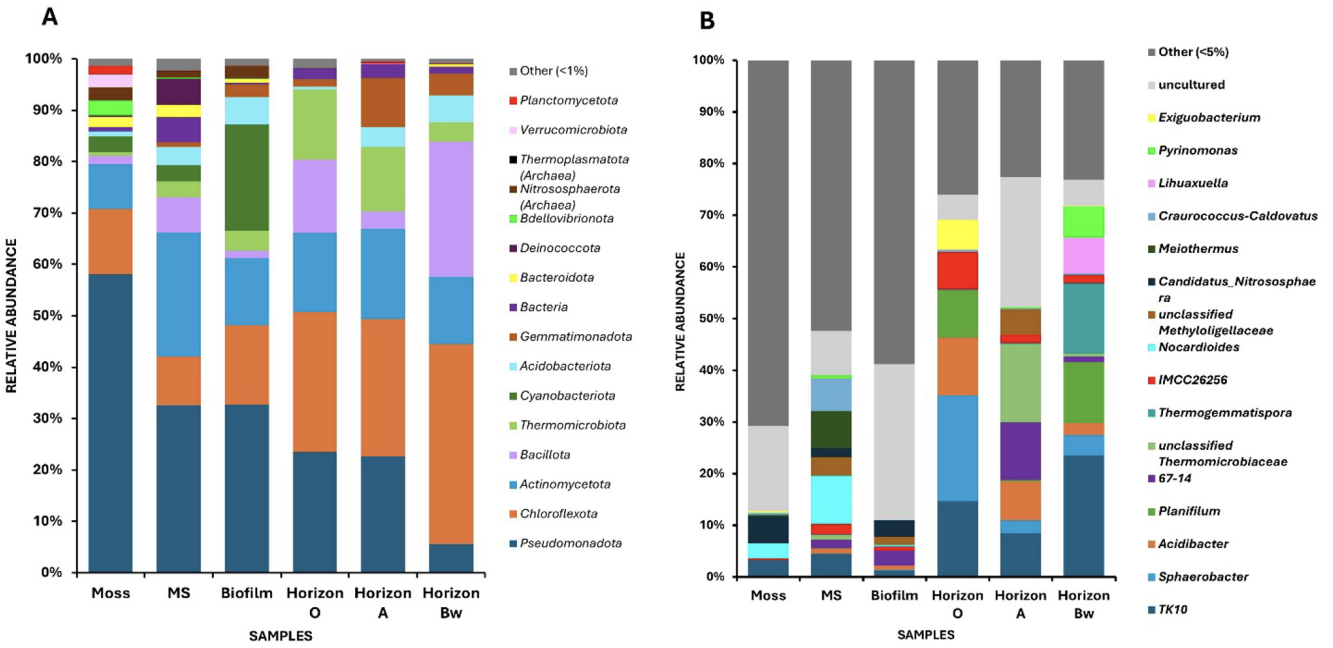


Figure 6. Relative abundances of microbial phyla **(A)** and genera **(B)** across different samples collected from Moss, moss substrate (MS), Biofilm, and soil horizons (O, A and Bw) samples.

(Bryukhanov et al., 2024), dominating the Horizon A, MS and Biofilm samples.

Other bacterial genera identified greater than 1 % of relative abundance were *Aureimonas*, *Bosea*, *Hyphomonas*, *Legionella*, *Methylorubrum* and *Nordella* in the Moss sample; *Candidatus Halysiosphaera*, *Limnobacter*, and *Chthonobacter* in the MS; *Dongia* in the Biofilm; and *Bauldia* in both the Biofilm and Horizon A, and *Brevundimonas* in both the Moss and MS samples. Notably, the genus *Bosea*, detected in the Moss sample, is known for its ability to obtain energy through the oxidation of reduced sulfur compounds, a process highly relevant in volcanic environments where sulfur-rich fumaroles, such as those produced during the Tajogaite eruption, have been documented (Martínez-Martínez et al., 2023).

The phylum *Chloroflexota* was also present in all samples and was particularly abundant in the O, A and Bw horizons, with relative abundances of 27.23 %, 26.77 % and 38.92 %, respectively. The most abundant members of this phylum were TK10, S085 and KD4-96, present in all samples along with the thermophilic bacteria *Thermogemmatispora* and *Litorilinea*, found predominantly in Horizon Bw and the Biofilm, respectively. Species of *Thermogemmatispora* are involved in carbon monoxide oxidation in geothermal environments (King and King, 2014). The *Candidatus Chloroploca*, found in the Moss, is capable of using sulfide oxidation as an electron donor (Gorlenko et al., 2014).

The *Actinomycetota* was the most abundant phylum in the MS sample, with the following genera being particularly prominent: *Nocardioides* (9.33 %), IMCC26256 (2.02 %), 67–14 (1.64 %), *Conexibacter* (1.23 %) and *Gaiella* (1.01 %). In the Biofilm, the *Micronomospora*, *Actinophytocola*, and 67–14 genera were the most abundant, with a relative abundance of 4.16 %, 1.81 %, and 2.94 %, respectively. In the soil horizons, thermophilic bacteria such as *Thermasporomyces* and *Thermopolyspora* (Horizon O) and *Thermoleophilum* (dominant in the Horizon Bw) were prevalent. Species of the *Thermopolyspora* genus are capable of degrading lignocellulosic compounds (Yang et al., 2022), which aligns with the detection of lignin exclusively in the Horizon O sample by Py-GC/MS. In contrast, members of the genus *Thermoleophilum* can grow exclusively on C_{12}–C_{19} *n*-alkanes, cyclohexane, cycloheptane, C_{12}–C_{18} alcohols and C_{13}–C_{19} ketones (Yakimov et al., 2003), all of which were identified in the soil samples through Py-GC/MS (Table S2).

The *Bacillota* was a dominant phylum in horizons Bw (26.29 %) and O (14.28 %), as well as in the MS sample (6.90 %). The most abundant genera within this phylum in the soil horizon samples were the thermophilic bacteria *Brockia*, *Thermaerobacter*, *Thermobacillus*, and *Lihuaxuella* (dominant in the Horizon Bw). The *Limnochorda* was found primarily in all three horizons, while *Planifilum*, dominant in horizons O and Bw, plays a key role in the degradation of organic matter and harbors potential antibiotic-resistance genes (Tseng et al., 2024). This genus was also found in the basaltic subsurface of young volcanic islands in Iceland (Bergsten et al., 2022). Non-thermophilic genera of the *Bacillota* phylum, such as *Exiguobacterium* and *Bacillus*, were also identified in all three sample types.

The *Thermomicrobiota* phylum was present in all samples, particularly in horizons O (13.63 %) and A (12.53 %), mainly represented by the *Sphaerobacter* genus, which was found in the three soil horizons, with particularly high dominance in Horizon O (20.51 %). This bacterium was originally isolated from thermophilically treated sludge, and proteogenomic analysis indicated that it contains numerous aromatic degradation pathways, such as those involved in lignin degradation (D'haeseleer et al., 2013), suggesting its role in the breakdown of complex organic matter. Notably, lignin was detected in the Horizon O sample (Fig. 3), while aromatic compounds have been detected in all samples (Fig. 3). The hyperthermophilic family *Thermomicrobiaceae* was also found, predominantly in Horizon A (15.11 %), represented by the 67–14 bacterium.

The *Cyanobacteriota* phylum was mainly found in the Biofilm (20.64 %), MS (3.07 %), and Moss (3.04 %) samples. Members of this phylum play a crucial role as nitrogen fixers and contribute significantly to the primary production of organic compounds (Rippin et al., 2018), as represented by genera such as *Arthronema* and *Nodosilinea*. This is consistent with the detection of nitrogen in the Biofilm, MS, and Moss samples, and supported by isotope ratios that predicted the presence of photosynthetic microorganisms. *Arthronema* is a filamentous cyanobacterium highly adaptive, typical of extreme desert environments, where it contributes to the nutritional chain and soil formation. Additionally, it exhibits antitumor and antioxidant properties and produces phycobiliproteins (Iliev and Andreeva, 2006; Chaneva et al., 2007; Gardeva et al., 2014; Petrova et al., 2020). Markers of proteins (peptides) were detected by Py-GC/MS in all samples, except MS. Although this technique cannot identify specific proteins, the presence of phycobiliproteins cannot be ruled out.

Other phyla identified in these samples included *Acidobacteriota*, mainly found in the Biofilm, MS and the A and Bw horizons; *Gemmatimonadota*, predominantly present in the Biofilm and soil horizon samples; and *Deinococcota* and *Bacteroidota*, primarily in the MS sample, represented by *Meiothermus* and *Persicitalea*. The *Deinococcota* phylum is known as one of the most extremophilic phyla of bacteria, due to its resistance to extreme stressors such as oxidation, radiation, desiccation, and high temperature (Vilhelmsson et al., 2023).

Thermophilic and thermotolerant bacteria constitute one of the most ecologically relevant features of this tephra-soil system and may reflect a potential influence of the persistent geothermal influence affecting the sampled profile. Their marked abundance in horizons O and Bw, as well as in the biofilm, may suggest that residual heat and fumarolic activity associated with the Tajogaite volcanic system continue to shape microbial community assembly two years after the eruption. This interpretation is particularly meaningful because thermophilic lineages were detected across multiple compartments of the profile rather than being restricted to a single layer, indicating that thermal disturbance has influenced both surface-associated and buried soil communities (Picone et al., 2020; Hernández et al., 2020).However, as this study was conducted at a single site near a fumarole, the potential influence of geothermal activity on the distribution of thermophilic taxa cannot be conclusively established without comparisons with non-fumarolic sites.

Several of the genera identified in these samples, including *Thermasporomyces*, *Thermopolyspora*, *Thermobacillus*, *Thermoleophilum*, *Sphaerobacter*, *Thermogemmatispora* and *Litorilinea*, are thermophilic bacteria known to participate in the degradation of lignocellulosic substrates, hydrocarbons and other structurally complex organic compounds. Their distribution is therefore consistent with the molecular patterns identified by Py-GC/MS (Fig. 3). In particular, the presence of lignin-derived compounds in Horizon O and the occurrence of PAHs and related aromatic compounds across the soil profile suggest that these microorganisms may be actively involved in the turnover and transformation of organic matter under geothermal influence. In this context, thermophiles should not be viewed merely as passive indicators of elevated temperature, but as potential drivers of biogeochemical processing during the early stages of soil recovery after tephra deposition (Nzila, 2018).

Their ecological relevance is further supported by the observed coexistence of thermophilic (e.g., *Thermasporomyces*, *Thermopolyspora*, *Thermobacillus*) and non-thermophilic (e.g., *Acidobacter*, *Norcadioides*, *Planifium*) taxa, which points to a dynamic microbial system structured by fluctuating thermal conditions rather than by permanently extreme temperatures. Such variability is consistent with the environmental monitoring data, which showed notable temporal oscillations in temperature and humidity at the sampling site. Temperature and humidity were continuously monitored over one year using a HOBO sensor. During this period, temperatures generally fluctuated between 20 and 30 °C, with the highest temperature (51.33 °C) recorded on 12 August and the lowest (13.76 °C) recorded on 24 February (Fig. S1B). The highest temperatures always coincided with the periods of lowest humidity. This combination of thermal heterogeneity, newly deposited volcanic material, and fresh organic inputs from mosses and biofilms likely creates a mosaic of ecological niches that favours functionally diverse microbial assemblages. Altogether, these results support the view that geothermal influence not only selects for specialized microbial taxa, but may also accelerate organic matter transformation, nutrient recycling and the first stages of andisol development in this recently disturbed volcanic environment (Guo et al., 2014; Hernández et al., 2020).

3.5 Linkages between biogeochemical data and microbial community composition

To synthesize the coupled patterns observed in the molecular (Py-GC/MS), elemental (% C and % N), and 16S rRNA datasets, we explored the ordination space defined by the PCoA biplot (Fig. 7). The first two axes captured over 85 % of the multivariate structure (PCo1 = 69.13 %; PCo2 = 19.03 %), revealing a dominant compositional gradient that separates the surface colonization system (Moss–Biofilm–moss substrate, MS) from the mineral soil horizons and, within the latter, differentiates the deeper horizon (H-Bw) from the upper layers (H-O and H-A). PCo1 (69.13 %) represents a major change from surface-associated, phototrophy-linked communities and labile biopolymers to soil-horizon assemblages associated with more processed and thermally-influenced organic pools. On the negative side of PCo1, the Moss sample plots together with vectors for *Cyanobacteriota* and *Bdellovibrionota*, consistent with a surface microbiome shaped by primary production and early successional colonizers. *Cyanobacteriota* are most prominent in the Biofilm and are also present in Moss and MS, supporting a role for photosynthetic microorganisms as early sources of organic inputs and nitrogen to the developing system (Rippin et al., 2018). In the same direction, the biplot loads polysaccharides (POL) and peptides (PEP) toward positive PCo2 but negative/near-zero PCo1, matching the expectation that extracellular polymeric substances and proteinaceous biomarkers contribute strongly to surface/interface organic matter (Palma et al., 2024). This interpretation is aligned with the biofilm chemistry, since the molecular composition of Biofilm is characterized by abundant lipids and aromatics but also a substantial polysaccharide and peptide fraction (Fig. 3), together with high C and N contents (Table 1). Conversely, the positive side of PCo1 is driven by soil-horizon taxa and organic families that indicate stronger transformation and/or thermal overprinting. The deepest horizon (H-Bw) is displaced toward the vectors of *Chloroflexota* and *Bacillota*, two phyla reported as dominant in the soil horizons (with *Chloroflexota* especially abundant in O, A and Bw, Fig. 6). This association is coherent with the ecological roles, since thermophilic and thermotolerant groups in these horizons are linked to degradation of complex organic substrates and hydrocarbons under geothermal influence near fumarolic activity (King and King, 2014). The same positive-PCo1 space is also aligned with aromatic compounds (ARO), nitrogen-containing compounds (N-Comp) and PAHs, consistent with the Py-GC/MS evidence that condensed aromatics/PAHs are particularly enhanced in the upper mineral horizon (A), reflecting pyrogenic inputs and/or strong thermal processing (Fig. 3). Importantly, several of the genera discussed in the paper (e.g., *Thermomicrobiota* representatives such as *Sphaerobacter*) are known to encode aromatic degradation pathways, providing a mechanistic link between the enrichment in aromatic/PAH-like pools and the microbial potential for their turnover (D'haeseleer et al., 2013). PCo2 (19.03 %) separates biopolymer-rich signatures from lipid/sterane and bulk-elemental signals, helping to distinguish the interface substrates from the more recalcitrant or source-specific pools. Positive PCo2 is dominated by POL and PEP, while negative PCo2 loads toward lipids (LIP) and steranes (STR), together with the elemental % C and % N vectors. In practice, this axis helps explain why Moss (and, to a lesser extent, the biofilm/interface samples) align with carbohydrate/protein-like inputs typical of fresh biomass and extracellular matrices. In contrast, the moss substrate (MS) shifts downward along PCo2, consistent with the strong plant-wax/lipid imprint described for MS (odd-dominated high-molecular-weight *n*-alkanes indicative of direct plant inputs; Fig. 4). Meanwhile, the sterane signal, preferentially preserved/accumulated in deeper horizons due to the stability of plant/fungal sterols and related compounds, supports the interpretation that part of the vertical separation reflects increasing preservation of recalcitrant biomarkers with depth.

The integrated PCoA supports a coherent conceptual model (Fig. 8) for this newly formed tephra–soil system: (i) moss establishment initiates a surface organic subsidy (biopolymers and labile inputs) and introduces/maintains phototrophy-linked taxa; (ii) at the interface, biofilms act as a biochemical and ecological "bridge", concentrating C and N and sustaining a mixed community consistent with rapid microbial assembly, and (iii) in the mineral horizons, particularly under geothermal influence, microbial communities change toward phyla and thermophilic lineages associated with the transformation of lignocellulosic and hydrocarbon pools, matching the observed enrichment in aromatic and PAH-like compounds and the depth-dependent preservation of stable biomarkers.

4 Conclusions

This study provides new insights into the early stages of soil development following the deposition of volcanic tephra produced by the 2021 Tajogaite eruption (La Palma Island). The results show that moss colonizing the upper tephra layer contributes organic compounds that serve as carbon sources for microorganisms, promoting rapid microbial colonization of the recently deposited volcanic substrate within only two years after the eruption.

Molecular analyses revealed clear differences between the organic matter composition of the tephra layer and the underlying soil horizons. Horizon O displayed a distinctive hydrocarbon signature associated with both thermal alteration processes and active microbial transformation of organic matter, whereas the deeper soil horizons (A and Bw) retained alkane patterns characteristic of plant-derived inputs. The $\delta^{13}C$ isotopic signatures further support intense microbial processing of organic carbon in the upper soil horizon, indicating that

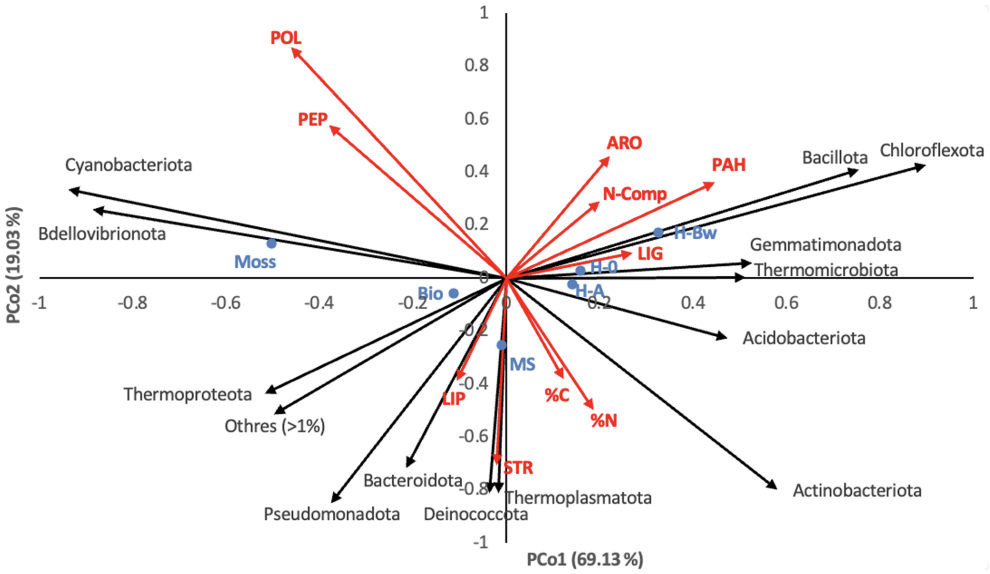


Figure 7. Combined principal coordinates analysis (PCoA) of the samples (blue labels) showing the projected loading weights of geochemical variables (red labels) and the most abundant phyla (black labels).

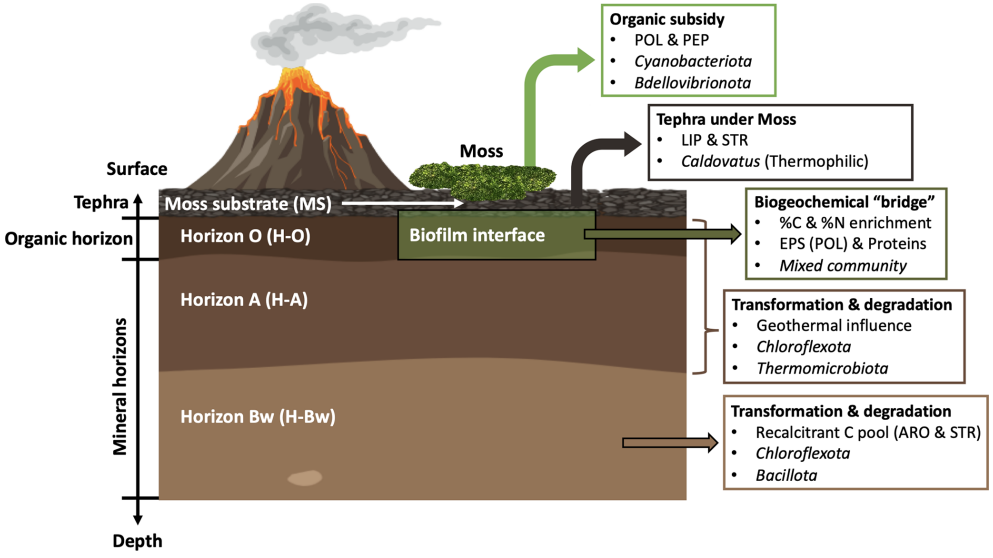


Figure 8. Integrated conceptual model of the tephra–soil system colonized by moss after volcanic deposition.

microbial activity plays a key role in the transformation of organic matter shortly after tephra deposition.

Microbial sequencing revealed the presence of *Cyanobacteriota* in the biofilm and surface-associated samples, highlighting the role of photosynthetic microorganisms as early colonizers contributing to primary production, nitrogen input, and substrate stabilization. The presence of ammonia-oxidizing archaea, sulfur-oxidizing bacteria, methane-utilizing microorganisms, ferric iron-reducing taxa, and hydrocarbon-metabolizing microorganisms, including members of the family *Methyloligellaceae*, indicates that key biogeochemical cycles were already active only two years after tephra deposition. In addition, the widespread presence of thermophilic microorganisms across the soil profile highlights the influence of geothermal activity associated with fumaroles in shaping microbial community composition and promoting the degradation of complex organic compounds in these recently disturbed soils.

Overall, our results reveal marked differences in soil organic matter dynamics and microbial community structure within a recently tephra-covered soil system, consistent with an important role of fresh volcanic deposits in the early stages of soil development. These findings highlight the important role of thermophilic microorganisms and pioneer

vegetation in driving the initial development of andisols and the recovery of soil ecosystems following volcanic disturbances.

To our knowledge, this is the first study integrating molecular pyrolysis, isotopic analysis and microbial sequencing to characterize the early biogeochemical transformation of tephra deposits after the Tajogaite eruption. Future studies monitoring the same tephra deposits over time will be essential to better understand the long-term evolution of organic matter transformation and microbial succession during andisol formation in volcanic environments.

Code availability. The bioinformatic analyses were performed using publicly available third-party software, including QIIME 2 (version 2024.5) and DADA2 through the q2-dada2 plugin. These tools are appropriately cited in the manuscript (https://doi.org/10.1038/S41587-019-0209-9, Bolyen et al., 2019; https://doi.org/10.1038/nmeth.3869, Callahan et al., 2016). No new standalone software was developed specifically for this study.

Data availability. The raw 16S rRNA gene amplicon sequencing data generated in this study have been deposited in the NCBI Sequence Read Archive (SRA) under BioProject accession number PRJNA1192049. The molecular, elemental, and isotopic data supporting the findings of this study are provided in the Supplementary Material. Additional data are available from the corresponding authors upon reasonable request.

Supplement. The supplement related to this article is available online at https://doi.org/10.5194/bg-23-8319-2026-supplement.

Author contributions. The manuscript was written through the contributions of all authors. All authors have approved the final version of the manuscript. S.G-P: data curation, formal analysis, methodology, visualization, writing–original draft. A.G.A.: data curation, formal analysis, methodology, visualization, writing–original draft. P.N-J.: methodology, validation, writing–original draft. J.M.-S.: methodology, validation, writing–review and editing. J.M-M.: methodology, validation, writing–review and editing. B.M-H.: methodology, writing–review and editing. J.V.: methodology, validation, writing–review and editing. N.T.J.-M.: data curation, formal analysis, methodology, visualization, validation, writing–original draft, writing–review and editing. A.Z.M.: data curation, formal analysis, methodology, validation, visualization, supervision, funding acquisition, writing–original draft, writing–review and editing.

Competing interests. The contact author has declared that none of the authors has any competing interests.

Disclaimer. Publisher's note: Copernicus Publications remains neutral with regard to jurisdictional claims made in the text, published maps, institutional affiliations, or any other geographical representation in this paper. The authors bear the ultimate responsibility for providing appropriate place names. Views expressed in the text are those of the authors and do not necessarily reflect the views of the publisher.

Acknowledgements. The authors are grateful to José Heriberto López, forest officer at the Caldera de Taburiente National Park (La Palma, Spain) for providing logistical support during the sampling campaign. All sampling campaigns were carried out under permits issued by the Cabildo de La Palma (Plan Territorial Insular de Emergencias de Protección Civil de la Isla de La Palma). We also acknowledge the support of CECOPIN and the PEINPAL (Cabildo de La Palma) and PEVOLCA (Government of the Canary Islands).

Financial support. This work received support from the Spanish Ministry of Science, Innovation and Universities (MICIU) under the research projects HIRES-SOM (grant no. TED2021-130683B-C21/C22), FIRE2C (grant no. CNS2023-143750), and HERMES (grant no. PID2024-162087NB-C21) funded by MCIN/AEI/10.13039/501100011033 and the European Union "NextGenerationEU"/PRTR. The research project MICROLAVA (grant no. PROYEXCEL_00185), funded by Junta de Andalucia is also acknowledged. N.T. Jiménez-Morillo acknowledges the "Ramón y Cajal" contract (grant no. RYC2021-031253-I) funded by MCIN/AEI/10.13039/501100011033 and the European Union "NextGenerationEU"/PRTR. A. Gómez-Arias acknowledges the "Juan de la Cierva" contract (grant no. JDC2022-049199-I) and the European Union "NextGenerationEU"/PRTR, and DGP_POST_2024_01054 contract funded by Junta de Andalucía/CUII and FSE+.

The article processing charges for this open-access publication were covered by the CSIC Open Access Publication Support Initiative through its Unit of Information Resources for Research (URICI).

Review statement. This paper was edited by Pierre Amato and reviewed by two anonymous referees.

References

Ågren, G. I., Bosatta, E., and Balesdent, J.: Isotope discrimination during decomposition of organic matter: A theoretical analysis, Soil Sci. Soc. Am. J., 60, 1121–1126, https://doi.org/10.2136/sssaj1996.03615995006000040023x, 1996.

Arias, M. E., González-Pérez, J. A., González-Vila, F. J., and Ball, A. S.: Soil health – a new challenge for microbiologists and chemists, Int. Microbiol., 8, 13–21, 2005.

Arnalds, O.: The influence of volcanic tephra (ash) on ecosystems, in: Advances in Agronomy, edited by: Sparks, D. L., Academic Press, 121, 331–380, https://doi.org/10.1016/B978-0-12-407685-3.00006-2, 2013.

Aznar, J. M., González-Pérez, J. A., Badía, D., and Martí, C.: At what depth are the properties of a gypseous forest topsoil affected by burning? Land. Degrad. Dev., 27, 1344–1353, https://doi.org/10.1002/ldr.2258, 2016.

Bergsten, P., Vannier, P., Frion, J., Mougeolle, A., and Marteinsson, V. Þ.: Culturable bacterial diversity from the basaltic subsurface of the young volcanic island of Surtsey, Iceland, Microorganisms, 10, 1177, https://doi.org/10.3390/microorganisms10061177, 2022.

Biass, S., Reyes-Hardy, M. P., Gregg, C., Di Maio, L. S., Dominguez, L., Frischknecht, C., Bonadonna, C., and Perez, N.: The spatiotemporal evolution of compound impacts from lava flow and tephra fallout on buildings: lessons from the 2021 Tajogaite eruption (La Palma, Spain), B. Volcanol., 86, 10, https://doi.org/10.1007/s00445-023-01700-w, 2024.

Billings, S. A. and Richter, D. D.: Changes in stable isotopic signatures of soil nitrogen and carbon during 40 years of forest development, Oecologia, 148, 325–333, https://doi.org/10.1007/s00442-006-0366-7, 2006.

Birnbaum, J., Lev, E., Hernandez, P. A., Barrancos, J., Padilla, G. D., Asensio-Ramos, M., Calvo, D., Rodríguez, F., Pérez, N. M., D'Auria, L., and Calvari, S.: Temporal variability of explosive activity at Tajogaite volcano, Cumbre Vieja (Canary Islands), 2021 eruption from ground-based infrared photography and videography, Front. Earth Sci., 11, https://doi.org/10.3389/feart.2023.1193436, 2023.

Bolyen, E., Rideout, J. R., Dillon, M. R., Bokulich, N. A., Abnet, C. C., Al-Ghalith, G. A., Alexander, H., Alm, E. J., Arumugam, M., Asnicar, F., Bai, Y., Bisanz, J. E., Bittinger, K., Brejnrod, A., Brislawn, C. J., Brown, C. T., Callahan, B. J., Caraballo-Rodríguez, A. M., Chase, J., Cope, E. K., Da Silva, R., Diener, C., Dorrestein, P. C., Douglas, G. M., Durall, D. M., Duvallet, C., Edwardson, C. F., Ernst, M., Estaki, M., Fouquier, J., Gauglitz, J. M., Gibbons, S. M., Gibson, D. L., Gonzalez, A., Gorlick, K., Guo, J., Hillmann, B., Holmes, S., Holste, H., Huttenhower, C., Huttley, G. A., Janssen, S., Jarmusch, A. K., Jiang, L., Kaehler, B. D., Kang, K. B., Keefe, C. R., Keim, P., Kelley, S. T., Knights, D., Koester, I., Kosciolek, T., Kreps, J., Langille, M. G. I., Lee, J., Ley, R., Liu, Y. X., Loftfield, E., Lozupone, C., Maher, M., Marotz, C., Martin, B. D., McDonald, D., McIver, L. J., Melnik, A. V., Metcalf, J. L., Morgan, S. C., Morton, J. T., Naimey, A. T., Navas-Molina, J. A., Nothias, L. F., Orchanian, S. B., Pearson, T., Peoples, S. L., Petras, D., Preuss, M. L., Pruesse, E., Rasmussen, L. B., Rivers, A., Robeson, M. S., Rosenthal, P., Segata, N., Shaffer, M., Shiffer, A., Sinha, R., Song, S. J., Spear, J. R., Swafford, A. D., Thompson, L. R., Torres, P. J., Trinh, P., Tripathi, A., Turnbaugh, P. J., Ul-Hasan, S., van der Hooft, J. J. J., Vargas, F., Vázquez-Baeza, Y., Vogtmann, E., von Hippel, M., Walters, W., Wan, Y., Wang, M., Warren, J., Weber, K. C., Williamson, C. H. D., Willis, A. D., Xu, Z. Z., Zaneveld, J. R., Zhang, Y., Zhu, Q., Knight, R., and Caporaso, J. G.: Reproducible, interactive, scalable and extensible microbiome data science using QIIME 2, Nat. Biotechnol. 37, 852–857, https://doi.org/10.1038/S41587-019-0209-9, 2019.

Bonadonna, C., Pistolesi, M., Biass, S., Voloschina, M., Romero, J., Coppola, D., Folch, A., D'Auria, L., Marrin-Lorenzo, A., Dominguez, L., Pastore, C., Reyes Hardy, M. P., and Rodriguez, F.: Physical characterization of long-lasting hybrid eruptions: The 2021 tajogaite eruption of cumbre vieja (La Palma, Canary Islands). J. Geophys. Res-Solid Ea., 127, 11, https://doi.org/10.1029/2022JB025302, 2022.

Bonadonna, C., Pistolesi, M., Dominguez, L., Freret-Lorgeril, V., Rossi, E., Fries, A., Biass, S., Voloschina, M., Lemus, J., Romero, J. E., Zanon, V., Pastore, C., Reyes Hardy, M.-P., Di Maio, L. S., Gabellini, P., Martin-Lorenzo, A., Rodriguez, F., and Perez, N. M.: Tephra sedimentation and grainsize associated with pulsatory activity: the 2021 Tajogaite eruption of Cumbre Vieja (La Palma, Canary Islands, Spain). Front. Earth Sci., 11, 1166073, https://doi.org/10.3389/feart.2023.1166073, 2023.

Bryukhanov, A. L., Sevastyanov, V. S., Kravchishina, M. D., Voropaev, S. A., Dushenko, N. V., Kurakov, A. V., and Fedulova, V. Y.: Composition of methane cycle microbial communities in the upper layers of bottom sediments of the Kara sea, Geochem. Int., 62, 609–617, https://doi.org/10.1134/S0016702924700277, 2024.

Bull, I. D., Nott, C. J., Van Bergen, P. F., Poulton, P. R., and Evershed, R. P.: Organic geochemical studies of soils from the Rothamsted classical experiments VI. The occurrence and source of organic acids in an experimental grassland soil, Soil Biol. Biochem., 32, 1367–1376, 2000.

Cabianca, A., Müller, L., Pawlowski, K., and Dahlin, P.: Changes in the plant β-sitosterol/stigmasterol ratio caused by the plant parasitic nematode meloidogyne incognita, Plants, 10, 1–15, https://doi.org/10.3390/plants10020292, 2021.

Callahan, B. J., McMurdie, P. J., Rosen, M. J., Han, A. W., Johnson, A. J. A., and Holmes, S. P.: DADA2: High-resolution sample inference from Illumina amplicon data, Nat. Methods, 13, 581–583, https://doi.org/10.1038/nmeth.3869, 2016.

Campeny, M., Menéndez, I., Ibáñez-Insa, J., Rivera-Martínez, J., Yepes, J., Álvarez-Pousa, S., Méndez-Ramos, J., and Mangas, J.: The ephemeral fumarolic mineralization of the 2021 Tajogaite volcanic eruption (La Palma, Canary Islands, Spain), Sci. Rep., 13, 6336, https://doi.org/10.1038/s41598-023-33387-6, 2023.

Capaccioni, B., Martini, M., and Mangani, F.: Light hydrocarbons in hydrothermal and magmatic fumaroles: hints of catalytic and thermal reactions, B. Volcanol., 56, 593–600, 1995.

Carracedo, J. C., Badiola, E. R., Guillou, H., de la Nuez, J., and Pérez-Torrado, F. J.: Geology and volcanology of la Palma and El Hierro, Estud. Geol., 57, 175–273, 2001.

Carracedo, J. C., Troll, V. R., Day, J. M. D., Geiger, H., Aulinas, M., Soler, V., Deegan, F. M., Perez-Torrado, F. J., Gisbert, G., Gazel, E., Rodriguez-Gonzalez, A., and Albert, H.: The 2021 eruption of the Cumbre Vieja volcanic ridge on La Palma, Canary Islands, Geology Today, 38, 94–107, https://doi.org/10.1111/gto.12388, 2022.

Carrell, A. A., Veličković, D., Lawrence, T. J., Bowen, B. P., Louie, K. B., Carper, D. L., Chu, R. K., Mitchell, H. D., Orr, G., Markillie, L. M., Jawdy, S. S., Grimwood, J., Shaw, A. J., Schmutz, J., Northen, T. R., Anderton, C. R., Pelletier, D. A., and Weston, D. J.: Novel metabolic interactions and environmental conditions mediate the boreal peatmoss-cyanobacteria mutualism, ISME J., 16, 1074–1085, https://doi.org/10.1038/s41396-021-01136-0, 2022.

Chaneva, G., Furnadzhieva, S., Minkova, K., and Lukavsky, J.: Effect of light and temperature on the cyanobacterium *Arthronema africanum* – A prospective phycobiliprotein-producing strain, J. Appl. Phycol., 19, 537–544, https://doi.org/10.1007/s10811-007-9167-6, 2007.

Chen, J., Zheng, Y., Guo, Y., Li, F., Xu, D., Chao, L., Qu, H., Wang, B., Ma, X., Wang, S., and Bao, Y.: Differences in microbial communities from Quaternary volcanic soils at different stages of development: Evidence from Late Pleistocene and Holocene volcanoes, Catena, 201, https://doi.org/10.1016/j.catena.2021.105211, 2021.

Craig, H., Wilson, T., Stewart, C., Outes, V., Villarosa, G., and Baxter, P.: Impacts to agriculture and critical infrastructure in Argentina after ashfall from the 2011 eruption of the Cordón Caulle volcanic complex: An assessment of published damage and function thresholds, J. Appl. Volcanol., 5, 7, https://doi.org/10.1186/s13617-016-0046-1, 2016.

de Blas, E., Almendros, G., and Sanz, J.: Molecular characterization of lipid fractions from extremely water-repellent pine and eucalyptus forest soils, Geoderma, 206, 75–84, https://doi.org/10.1016/j.geoderma.2013.04.027, 2013.

De la Rosa, J. M., Jiménez-Morillo, N. T., González-Pérez, J. A., Almendros, G., Vieira, D., Knicker, H. E., and Keizer, J.: Mulching-induced preservation of soil organic matter quality in a burnt eucalypt plantation in central Portugal, J. Environ. Manage., 231, 1135–1144, https://doi.org/10.1016/j.jenvman.2018.10.114, 2019.

De la Rosa, J. M., Pérez-Dalí, S. M., Campos, P., Sánchez-Martín, Á., González-Pérez, J. A., and Miller, A. Z.: Suitability of volcanic ash, rice husk ash, green compost and biochar as amendments for a Mediterranean alkaline soil, Agronomy, 13, 4, https://doi.org/10.3390/agronomy13041097, 2023.

D'haeseleer, P., Gladden, J. M., Allgaier, M., Chain, P. S. G., Tringe, S. G., Malfatti, S. A., Aldrich, J. T., Nicora, C. D., Robinson, E. W., Paša-Tolić, L., Hugenholtz, P., Simmons, B. A., and Singer, S. W.: Proteogenomic analysis of a thermophilic bacterial consortium adapted to deconstruct switchgrass, PLOS One, 8, https://doi.org/10.1371/journal.pone.0068465, 2013.

Dragone, N. B., Whittaker, K., Lord, O. M., Burke, E. A., Dufel, H., Hite, E., Miller, F., Page, G., and Slayback, D.: The early microbial colonizers of a short-lived volcanic island in the Kingdom of Tonga, mBio, 14, 1, https://doi.org/10.1128/mbio.03313-22, 2023.

Ehleringer, J. R., Buchmann, N., and Flanagan, L. B.: Carbon isotope ratios in belowground carbon cycle processes, Ecol. Appl., 10, 412–422, https://doi.org/10.2307/2641103, 2000.

Falagán, C. and Johnson, D. B.: *Acidibacter ferrireducens* gen. nov., sp. nov.: an acidophilic ferric iron-reducing gammaproteobacterium, Extremophiles, 18, 1067–1073, https://doi.org/10.1007/s00792-014-0684-3, 2014.

Feakins, S. J, Peters, T., Wu, M. S., Shenkin, A., Salinas, N., Girardin, C. A. J., Bentley, L. P., Blonder, B., Enquist, B. J., Martin, R. E., Asner, G. P., and Malhi, Y.: Production of leaf wax *n*-alkanes across a tropical forest elevation transect, Org. Geochem., 100, 89–100, https://doi.org/10.1016/j.orggeochem.2016.07.004, 2016.

Ferrer, N., Marrero-Rodríguez, N., Sanromualdo-Collado, A., Vegas, J., and García-Romero, L.: Early morphodynamics of the sudden formation of beaches during the 2021 volcanic eruption of La Palma, Geomorphology, 436, https://doi.org/10.1016/j.geomorph.2023.108779, 2023.

Fraser, C. M. and Chapple, C.: The phenylpropanoid pathway in *Arabidopsis*, Arabidopsis Book, 9, e0152, https://doi.org/10.1199/tab.0152, 2011.

Fujimura, R., Kim, S. W., Sato, Y., Oshima, K., Hattori, M., Kamijo, T., and Ohta, H.: Unique pioneer microbial communities exposed to volcanic sulfur dioxide, Sci. Rep., 6, 19687, https://doi.org/10.1038/srep19687, 2016.

Gardeva, E. G., Toshkova, R. A., Yossifova, L. S., Minkova, K., Ivanova, N. Y., and Gigova, L. G.: Antitumor activity of C-phycocyanin from *Arthronema africanum* (Cyanophyceae), Braz. Arch. Biol. Techn., 57, 675–684, https://doi.org/10.1590/S1516-89132014005000018, 2014.

Ghezzi, D., Jiménez-Morillo, N. T., Foschi, L., Donini, E., Chiarini, V., De Waele, J., Miller, A. Z., and Cappelletti, M.: The microbiota characterizing huge carbonatic moonmilk structures and its correlation with preserved organic matter, Environmental Microbiome, 19, 25, https://doi.org/10.1186/s40793-024-00562-9, 2024.

Girona-García, A., Badía-Villas, D., Jiménez-Morillo, N. T., de la Rosa, J. M., and González-Pérez, J. A.: Soil C and N isotope composition after a centennial Scots pine afforestation in podzols of native European beech forests in NE-Spain, Catena, 165, 434–441, https://doi.org/10.1016/j.catena.2018.02.023, 2018.

González-Pérez, J. A., Almendros, G., De La Rosa, J. M., and González-Vila, F. J.: Appraisal of polycyclic aromatic hydrocarbons (PAHs) in environmental matrices by analytical pyrolysis (Py-GC/MS), J. Anal. Appl. Pyrol., 109, 1–8, https://doi.org/10.1016/j.jaap.2014.07.005, 2014.

González-Pérez, J. A., Jiménez-Morillo, N. T., de la Rosa, J. M., Almendros, G., and González-Vila, F. J.: Compound-specific stable carbon isotopic signature of carbohydrate pyrolysis products from C3 and C4 plants, J. Sci. Food. Agric., 96, 948–953, https://doi.org/10.1002/jsfa.7169, 2016.

Gorlenko, V. M., Bryantseva, I. A., Kalashnikov, A. M., Gaisin, V. A., Sukhacheva, M. V., Gruzdev, D. S., and Kuznetsov, B. B.: *Candidatus 'Chloroploca asiatica'* gen. nov., sp. nov., a new mesophilic filamentous anoxygenic phototrophic bacterium, Microbiology, 83, 838–848, https://doi.org/10.1134/S0026261714060083, 2014.

Guo, Y., Fujimura, R., Sato, Y., Suda, W., Kim, S. W., Oshima, K., Hattori, M., Kamijo, T., Narisawa, K., and Ohta, H.: Characterization of early microbial communities on volcanic deposits along a vegetation gradient on the island of Miyake, Japan, Microbes Environ., 29, 38–49, https://doi.org/10.1264/jsme2.me13142, 2014.

Gutierrez-Patricio, S., Osman, J. R., Luis Gonzalez-Pimentel, J., Jurado, V., Laiz, L., Laínez Concepción, A., Saiz-Jimenez, C., and Miller, A. Z.: Microbiological exploration of the Cueva del Viento lava tube system in Tenerife, Canary Islands, Env. Microbiol. Rep., 16, e13245, https://doi.org/10.1111/1758-2229.13245, 2024.

Habib, N., Khan, I. U., Hussain, F., Zhou, E. M., Xiao, M., Ahmed, I., Zhi, X. Y., and Li, W. J.: *Caldovatus sediminis* gen. nov., sp. nov., a moderately thermophilic bacterium isolated from a hot spring, Int. J. Syst. Evol. Microbiol., 67, 4716–4721, https://doi.org/10.1099/ijsem.0.002363, 2017.

Hernández, M., Calabi, M., Conrad, R., and Dumont, M. G.: Analysis of the microbial communities in soils of different ages following volcanic eruptions, Pedosphere, 30, 1, 126–134, https://doi.org/10.1016/S1002-0160(19)60823-4, 2020.

Hernández, Z., Almendros, G., Carral, P., Álvarez, A., Knicker, H., and Pérez-Trujillo, J. P.: Influence of non-crystalline miner-

als in the total amount, resilience and molecular composition of the organic matter in volcanic ash soils (Tenerife Island, Spain), Eur. J. Soil Sci., 63, 603–615, https://doi.org/10.1111/j.1365-2389.2012.01497.x, 2012.

Hoernle, K. A. J., and Carracedo, J. C.: Canary Islands geology, University of California Press, ISBN 978-0-5202-5649-1, 2009.

Högberg, P.: Tansley review no. 95 natural abundance in soil-plant systems, New Phytol., 137, 179–203, https://doi.org/10.1046/j.1469-8137.1997.00808.x, 1997.

Hu, C. J., Xian, W. D., Lv, Y. Q., Peng, C. X., Shan, R. X., Cheng, Z. C., Lv, Q., Tian, Y., Jiao, J. Y., Tan, S., and Li, W. J.: *Caldovatus aquaticus* sp. nov., a moderately thermophilic bacterium isolated from hot spring microbial mat, Int. J. Syst. Evol. Microbiol., 72, 5627, https://doi.org/10.1099/ijsem.0.005627, 2022.

Iliev, I. P. G. D. and Andreeva, R.: Membrane metabolites of *Arthronema africanum* strains from extreme habitats, Gen. Appli. Plant. Physiology, 32, 117–123, 2006.

Ingimundardóttir, G. V., Weibull, H., and Cronberg, N.: Bryophyte colonization history of the virgin volcanic island Surtsey, Iceland, Biogeosciences, 11, 4415–4427, https://doi.org/10.5194/bg-11-4415-2014, 2014.

Iwasaki, S., Endo, Y., Hatano, R., and Toma, Y.: Factors impacting soil organic carbon pool in different types of Andosols in Toya, Hokkaido, Japan, Soil Sci. Plant. Nutr., 67, 594–605, https://doi.org/10.1080/00380768.2021.1959836, 2021.

Jaffé, R., Elismé, T., and Cabrera, A. C.: Organic geochemistry of seasonally flooded rain forest soils: molecular composition and early diagenesis of lipid components, Org. Geochem., 25, 9–17, 1996.

Jiménez-Morillo, N. T., de la Rosa, J. M., Waggoner, D., Almendros, G., González-Vila, F. J., and González-Pérez, J. A.: Fire effects in the molecular structure of soil organic matter fractions under *Quercus suber* cover, Catena, 145, 266–273, https://doi.org/10.1016/j.catena.2016.06.022, 2016a.

Jiménez-Morillo, N. T., González-Pérez, J. A., Jordán, A., Zavala, L. M., de la Rosa, J. M., Jiménez-González, M. A., and González-Vila, F. J.: Organic matter fractions controlling soil water repellency in sandy soils from the Doñana national park (Southwestern Spain), Land. Degrad. Dev., 27, 1413–1423, https://doi.org/10.1002/ldr.2314, 2016b.

Jiménez-Morillo, N. T., Spangenberg, J. E., Miller, A. Z., Jordán, A., Zavala, L. M., González-Vila, F. J., and González-Pérez, J. A.: Wildfire effects on lipid composition and hydrophobicity of bulk soil and soil size fractions under Quercus suber cover (SW-Spain), Environ. Res, 159, 394–405, https://doi.org/10.1016/j.envres.2017.08.022, 2017.

Jiménez-Morillo, N. T., González-Pérez, J. A., Almendros, G., De la Rosa, J. M., Waggoner, D. C., Jordán, A., Zavala, L. M., González-Vila, F. J., and Hatcher, P. G.: Ultra-high resolution mass spectrometry of physical speciation patterns of organic matter in fire-affected soils, J. Environ. Manage., 225, 139–147, https://doi.org/10.1016/j.jenvman.2018.07.069, 2018.

Jiménez-Morillo, N. T., Almendros, G., De la Rosa, J. M., Jordán, A., Zavala, L. M., Granged, A. J. P., and González-Pérez, J. A.: Effect of a wildfire and of post-fire restoration actions in the organic matter structure in soil fractions, Sci. Total Environ., 728, 138715, https://doi.org/10.1016/j.scitotenv.2020.138715, 2020a.

Jiménez-Morillo, N. T., Almendros, G., González-Vila, F. J., Jordán, A., Zavala, L. M., de la Rosa, J. M., and González-Pérez, J. A.: Fire effects on C and H isotopic composition in plant biomass and soil: Bulk and particle size fractions, Sci. Total Environ., 749, 141417, https://doi.org/10.1016/j.scitotenv.2020.141417, 2020b.

Jiménez-Morillo, N. T., Almendros, G., Miller, A. Z., Hatcher, P. G., and González-Pérez, J. A.: Hydrophobicity of soils affected by fires: An assessment using molecular markers from ultra-high resolution mass spectrometry, Sci. Total Environ., 817, 152957, https://doi.org/10.1016/j.scitotenv.2022.152957, 2022.

Katsumi, N., Yonebayashi, K., Fujitake, N., and Okazaki, M.: Relationship between stable carbon and nitrogen isotope ratios of humic acids extracted from Andisols and non-Andisols, Catena, 127, 214–221, https://doi.org/10.1016/j.catena.2015.01.005, 2015.

Kellner, H., Luis, P., Pecyna, M. J., Barbi, F., Kapturska, D., Krug¨er, D., Zak, D. R., Marmeisse, R., Vandenbol, M., and Hofrichter, M.: Widespread occurrence of expressed fungal secretory peroxidases in forest soils, PLOS One, 9, e95557, https://doi.org/10.1371/journal.pone.0095557, 2014.

King, C. E. and King, G. M.: Description of *Thermogemmatispora carboxidivorans* sp. nov., a carbon-monoxideoxidizing member of the class Ktedonobacteria isolated from a geothermally heated biofilm, and analysis of carbon monoxide oxidation by members of the class Ktedonobacteria, Int. J. Syst. Evol. Microbiol., 64, 1244–1251, https://doi.org/10.1099/ijs.0.059675-0, 2014.

Klavina, L., Springe, G., Nikolajeva, V., Martsinkevich, I., Nakurte, I., Dzabijeva, D., and Steinberga, I.: Molecules chemical composition analysis, antimicrobial activity and cytotoxicity screening of moss extracts (Moss Phytochemistry), Molecules, 20, 17221–17243, https://doi.org/10.3390/molecules200917221, 2015.

Klegin, C., Ethur, E. M., Bordin, J., and Baia Figueiredo, P. L.: Chemical composition of essential oil from mosses from the brazilian atlantic forest, Chem. Biodivers., 20, e202300286, https://doi.org/10.1002/cbdv.202300286, 2023.

Klindworth, A., Pruesse, E., Schweer, T., Peplies, J., Quast, C., Horn, M., and Glöckner, F. O.: Evaluation of general 16S ribosomal RNA gene PCR primers for classical and next-generation sequencing-based diversity studies, Nucleic Acids Res., 41, e1, https://doi.org/10.1093/nar/gks808, 2013.

Krauss, M., Wilcke, W., Martius, C., Bandeira, A. G., Garcia, M. V. B., and Amelung, W.: Atmospheric versus biological sources of polycyclic aromatic hydrocarbons (PAHs) in a tropical rain forest environment, Environ. Pollut., 135, 143–154, https://doi.org/10.1016/j.envpol.2004.09.012, 2005.

Kristan, K. and Rižner, T. L.: Steroid-transforming enzymes in fungi, J. Steroid. Biochem. Mol. Biol., 129, 79–91, https://doi.org/10.1016/j.jsbmb.2011.08.012, 2012.

Krüger, N., Finn, D. R., and Don, A.: Soil depth gradients of organic carbon-13 – A review on drivers and processes, Plant Soil, 495, 113–136, https://doi.org/10.1007/s11104-023-06328-5, 2024.

Kumar, M., Boski, T., González-Vila, F. J., Jiménez-Morillo, N. T., and González-Pérez, J. A.: Characteristics of organic matter sources from Guadiana Estuary salt marsh sediments (SW Iberian Peninsula), Cont. Shelf Res., 197, 104076, https://doi.org/10.1016/j.csr.2020.104076, 2020.

Ladygyna, N., Dedyukhina, E. G., and Vainshtein, M. B.: A review on microbial synthesis of hydrocarbons, Process Biochem.,

41, 1001–1014, https://doi.org/10.1016/j.procbio.2005.12.007, 2006.

Leal, O. A., Jiménez-Morillo, N. T., González-Pérez, J. A., Knicker, H., de Souza Costa, F., Jiménez-Morillo, P. N., de Carvalho Júnior, J. A., dos Santos, J. C., and Pinheiro Dick, D.: Soil organic matter molecular composition shifts driven by forest regrowth or pasture after slash-and-burn of amazon forest, Int. J. Env. Res. Pub. He., 20, 3485, https://doi.org/10.3390/ijerph20043485, 2023.

Lehtonen, K. and Ketola, M.: Occurrence of long-chain acyclic methyl ketones in *Sphagnum* and *Carex* peats of various degress of humification, Org. Geochem., 15, 275–280, https://doi.org/10.1016/0146-6380(90)90005-K, 1990.

Lehtovirta-Morley, L. E., Ge, C., Ross, J., Yao, H., Hazard, C., Gubry-Rangin, C., Prosser, J. I., and Nicol, G. W.: *Nitrosotalea devaniterrae* gen. nov., sp. nov. and *Nitrosotalea sinensis* sp. nov., two acidophilic ammonia oxidising archaea isolated from acidic soil, and proposal of the new order Nitrosotaleales ord. nov. within the class Nitrososphaeria of the phylum Nitrososphaerota, Int. J. Syst. Evol. Microbiol., 74, https://doi.org/10.1099/ijsem.0.006387, 2024.

Leininger, S., Urich, T., Schloter, M., Schwark, L., Qi, J., Nicol, G. W., Prosser, J. I., Schuster, S. C., and Schleper, C.: Archaea predominate among ammonia-oxidizing prokaryotes in soils, Nature, 442, 806–809, https://doi.org/10.1038/nature04983, 2006.

Longpré, M.-A. and Felpeto, A.: Historical volcanism in the Canary Islands; part 1: A review of precursory and eruptive activity, eruption parameter estimates, and implications for hazard assessment, J. Volcanol. Geoth. Res., 419, 107363, https://doi.org/10.1016/j.jvolgeores.2021.107363, 2021.

Love, C. R., Arrington, E. C., Gosselin, K. M., Reddy, C. M., Van Mooy, B. A. S., Nelson, R. K., and Valentine, D. L.: Microbial production and consumption of hydrocarbons in the global ocean, Nat. Microbiol., 6, 489–498, https://doi.org/10.1038/s41564-020-00859-8, 2021.

Makarov, M. I.: The nitrogen isotopic composition in soils and plants: Its use in environmental studies (A Review), Soil Chemistry, 42, 1335–1347, https://doi.org/10.1134/S1064229309120035, 2009.

Martínez-Espinosa, R. M.: Microorganisms and their metabolic capabilities in the context of the biogeochemical nitrogen cycle at extreme environments, Int. J. Mol. Sci., 21, 4228, https://doi.org/10.3390/ijms21124228, 2020.

Martínez-Martínez, J., Mediato, J. F., Mata, M. P., Ordóñez, B., del Moral, B., Bellido, E., Pérez-López, R., Rodríguez-Pascua, M. A., Vegas, J., Lozano Otero, G., Mateos, R. M., Sánchez, N., and Galindo, I.: Early fumarolic minerals from the Tajogaite volcanic eruption (La Palma, 2021), J. Volcanol. Geotherm. Res., 435, 107771, https://doi.org/10.1016/j.jvolgeores.2023.107771, 2023.

Matus, F., Rumpel, C., Neculman, R., Panichini, M., and Mora, M. L.: Soil carbon storage and stabilisation in andic soils: A review, Catena, 120, 102–110, https://doi.org/10.1016/j.catena.2014.04.008, 2014.

Miller, A. Z., De la Rosa, J. M., Jiménez-Morillo, N. T., Pereira, M. F. C., González-Pérez, J. A., Calaforra, J. M., and Saiz-Jimenez, C.: Analytical pyrolysis and light stable isotope analyses reveal environmental changes in coralloid speleothems from Easter Island (Chile), J. Chromatogr. A, 1461, 144–152, https://doi.org/10.1016/j.chroma.2016.07.038, 2016.

Miller, A. Z., De la Rosa, J. M., Jiménez-Morillo, N. T., Pereira, M. F. C., Gonzalez-Perez, J. A., Knicker, H., and Saiz-Jimenez, C.: Impact of wildfires on subsurface volcanic environments: New insights into speleothem chemistry, Sci. Total Environ., 698, https://doi.org/10.1016/j.scitotenv.2019.134321, 2020.

Miller, A. Z., Jiménez-Morillo, N. T., Coutinho, M. L., Gazquez, F., Palma, V., Sauro, F., Pereira, M. F. C., Rull, F., Toulkeridis, T., Caldeira, A. T., Forti, P., and Calaforra, J. M.: Organic geochemistry and mineralogy suggest anthropogenic impact in speleothem chemistry from volcanic show caves of the Galapagos, iScience, 25, 104556, https://doi.org/10.1016/j.isci.2022.104556, 2022.

Mohapatra, B. and Phale, P. S.: Microbial degradation of naphthalene and substituted naphthalenes: Metabolic diversity and genomic insight for bioremediation, Front. Bioeng. Biotechnol., 9, https://doi.org/10.3389/fbioe.2021.602445, 2021.

Muñoz, G., Orlando, J., and Zuñiga-Feest, A.: Plants colonizing volcanic deposits: root adaptations and effects on rhizosphere microorganisms, Plant Soil, 461, 265–279, https://doi.org/10.1007/s11104-020-04783-y, 2021.

Musat, F., Galushko, A., Jacob, J., Widdel, F., Kube, M., Reinhardt, R., Wilkes, H., Schink, B., and Rabus, R.: Anaerobic degradation of naphthalene and 2-methylnaphthalene by strains of marine sulfate-reducing bacteria, Environ. Microbiol., 11, 209–219, https://doi.org/10.1111/j.1462-2920.2008.01756.x, 2009.

Nanzyo, M., Dahlgren, R., and Shoji, S.: Chemical characteristics of volcanic ash soils, in: Shoji, S., Nanzyo, M., and Dahlgren, R., edited by: Volcanic Ash Soils – Genesis, Properties and Utilization, Developments in Soil Science, Elsevier, Amsterdam, 145–188, https://doi.org/10.1016/S0166-2481(08)70267-8, 1993.

Nierop, K. G. J. and Buurman, P.: Thermally assisted hydrolysis and methylation of organic matter in two allophanic volcanic ash soils from the Azores Islands, in: Soils of Volcanic Regions in Europe, edited by: Arnalds, O., óskarsson, H., Bartolini, F., Buurman, P., Stoops, G., García-Rodeja, E., Springer, Berlin, Heidelberg, https://doi.org/10.1007/978-3-540-48711-1_30, 2007.

Nzila, A.: Current status of the degradation of aliphatic and aromatic petroleum hydrocarbons by thermophilic microbes and future perspectives, Int. J. Env. Res. Pub. He., 15, 2782, https://doi.org/10.3390/ijerph15122782, 2018.

Offre, P., Spang, A., and Schleper, C.: Archaea in biogeochemical cycles, Annu. Rev. Microbiol., 67, 437–457, https://doi.org/10.1146/annurev-micro-092412-155614, 2013.

Palma, V., De la Rosa, J. M., Onac, B. P., Sauro, F., Martínez-Frías, J., Caldeira, A. T., González-Pérez, J. A., Jiménez-Morillo, N. T., and Miller, A. Z.: Decoding organic compounds in lava tube sulfates to understand potential biomarkers in the Martian subsurface, Commun. Earth Environ., 5, 530, https://doi.org/10.1038/s43247-024-01673-4, 2024.

Park, R. and Epstein, S.: Metabolic fractionation of C13 and C12 in plants, Plant Physiol., 36, 133–8, https//-doi.org/10.1104/pp.36.2.133, 1961.

Peng, X., Tamura, K., Asano, M., Takano, A., Kawagoe, M., and Kamijo, T.: Changes in soil physical and chemical properties during vegetation succession on miyake-jima island, Forests, 12, 1435, https://doi.org/10.3390/f12111435, 2021.

Petkova, Z., Teneva, O., Antova, G., Angelova-Romova, M., Gecheva, G., and Dimitrova-Dyulgerova, I.: Chemical composition, lipid-soluble bioactive compounds and potential health ben-

efits of the moss *Hypnum cupressiforme* Hedw, Plants, 12, 4190, https://doi.org/10.3390/plants12244190, 2023.

Petrova, D. H., Yocheva, L., and Petrova, M.: Antimicrobial and antioxidant activities of microalgal extracts, Oxid. Commun., 43, 103–116, https://doi.org/10.13140/RG.2.2.20509.84963, 2020.

Picone, N., Hogendoorn, C., Cremers, G., Poghosyan, L., Pol, A., van Alen, T. A., Gagliano, A. L., D'Alessandro, W., Quatrini, P., Jetten, M. S. M., Op den Camp, H. J. M, and Berben, T.: Geothermal gases shape the microbial community of the volcanic soil of Pantelleria, Italy, mSystems, 5, https://doi.org/10.1128/msystems.00517-20, 2020.

Quast, C., Pruesse, E., Yilmaz, P., Gerken, J., Schweer, T., Yarza, P., Peplies, J., and Glöckner, F. O.: The SILVA ribosomal RNA gene database project: Improved data processing and web-based tools, Nucleic Acids Res., 41, D590–D596, https://doi.org/10.1093/nar/gks1219, 2013.

Rabbi, S. M. F., Wilson, B. R., Lockwood, P. V., Daniel, H., and Young, I. M.: Soil organic carbon mineralization rates in aggregates under contrasting land uses, Geoderma, 216, 10–18, https://doi.org/10.1016/j.geoderma.2013.10.023, 2014.

Ramos, P., Honda, R., Hoek, E. M. V., and Mahendra, S.: Carbon/nitrogen ratios determine biofilm formation and characteristics in model microbial cultures, Chemosphere, 313, https://doi.org/10.1016/j.chemosphere.2022.137628, 2023.

Ren, G., Zhang, Y., Chen, Z., Xue, X., and Fan, H.: Research progress of small plant peptides on the regulation of plant growth, development, and abiotic stress, Int. J. Mol. Sci., 25, 4114, https://doi.org/10.3390/ijms25074114, 2024.

Renault, H., Alber, A., Horst, N. A., Lopes, A. B., Fich, E. A., Kriegshauser, L., Wiedemann, G., Ullmann, P., Herrgott, L., Erhardt, M., Pineau, E., Ehlting, J., Schmitt, M., Rose, J. K. C., Reski, R., and Werck-Reichhart, D.: A phenol-enriched cuticle is ancestral to lignin evolution in land plants, Nat. Commun., 8, 14713, https://doi.org/10.1038/ncomms14713, 2017.

Rippin, M., Borchhardt, N., Williams, L., Colesie, C., Jung, P., Büdel, B., Karsten, U., and Becker, B.: Genus richness of microalgae and Cyanobacteria in biological soil crusts from Svalbard and Livingston Island: morphological versus molecular approaches, Polar Biol., 41, 909–923, https://doi.org/10.1007/s00300-018-2252-2, 2018.

San-Emeterio, L. M., Zavala, L. M., Jiménez-Morillo, N. T., Pérez-Ramos, I. M., and González-Pérez, J. A.: Effects of climate change on soil organic matter C and H isotope composition in a Mediterranean Savannah (Dehesa): An assessment using Py-CSIA, Environ. Sci. Technol., 57, 13851–13862, https://doi.org/10.1021/acs.est.3c01816, 2023.

Sánchez-España, J. , Mata, M. P., Vegas, J., Lozano, G., Mediato, J., Martínez Martínez, J., Galindo, I., Sánchez, N., del Moral, B., Ordóñez, B., de Vergara, A., Nieto, A., Andrés, M., Vázquez, I., Bellido, E., and Castillo-Carrión, M.: Leaching tests reveal fast aluminum fluoride release from ashfall accumulated in La Palma (Canary Islands, Spain) after the 2021 Tajogaite eruption, J. Volcanol. Geoth. Res., 444, 107959, https://doi.org/10.1016/j.jvolgeores.2023.107959, 2023.

Schwark, L., Zink, K., and Lechterbeck, J.: Reconstruction of postglacial to early Holocene vegetation history in terrestrial Central Europe via cuticular lipid biomarkers and pollen records from lake sediments, Geology, 30, 463–466, https://doi.org/10.1130/0091-7613(2002)030<0463:ROPTEH>2.0.CO;2, 2002.

Smith, R. J. L.: Colonization by bryophytes following recent volcanic activity on an Antarctic island, J. Hattori Bot. Lab., 56, 53–63, 1984.

Sokolova, T. A.: Low-Molecular-Weight Organic Acids in Soils: Sources, Composition, Concentrations, and Functions: A Review, Eurasian Soil Sci., 53, 580–594, https://doi.org/10.1134/S1064229320050154, 2020.

Soil Survey Staff: Keys to Soil Taxonomy, 13th edn., USDA Natural Resources Conservation Service, ISBN-10 1998295001, 2022.

Szpak, P.: Complexities of nitrogen isotope biogeochemistry in plant-soil systems: Implications for the study of ancient agricultural and animal management practices, Front. Plant Sci., 5, https://doi.org/10.3389/fpls.2014.00288, 2014.

Taddeucci, J., Scarlato, P., Andronico, D., Ricci, T., Civico, R., Del Bello, E., Spina, L., D'Auria, L., Asensio-Ramos, M., Calvo, D., Padrón, E., Hernández, P. A., and Pérez, N. M.: The explosive activity of the 2021 Tajogaite Eruption (La Palma, Canary Islands, Spain), Geochem. Geophys. Geosyst., 24, https://doi.org/10.1029/2023GC010946, 2023.

Tomašek, I., Damby, D. E., Andronico, D., Baxter, P. J., Boonen, I., Claeys, P., Denison, M. S., Horwell, C. J., Kervyn, M., Kueppers, U., Romanias, M. N., and Elskens, M.: Assessing the biological reactivity of organic compounds on volcanic ash: implications for human health hazard, Bull. Volcanol., 83, https://doi.org/10.1007/s00445-021-01453-4, 2021.

Troll, V. R., Aulinas, M., Carracedo, J. C., Geiger, H., Perez-Torrado, F. J., Soler, V., Deegan, F. M., Bloszies, C., Weis, F., Albert, H., Gisbert, G., Day, J. M. D., Rodríguez-Gonzalez, A., Gazel, E., and Dayton, K.: The 2021 La Palma eruption: social dilemmas resulting from life close to an active volcano, Geology Today, 40, 96–111, https://doi.org/10.1111/gto.12472, 2024.

Tseng, H. C., Matsutani, M., Fujimoto, N., and Ohnishi, A.: Draft genome sequence and morphological data of *Planifilum fimeticola* PLACP1, a thermophilic chloramphenicol-resistant bacterium isolated from thermophilic sludge, Data Brief, 54, https://doi.org/10.1016/j.dib.2024.110447, 2024.

Ustiatik, R., Ariska, A. P., Hakim, Q. L., Wicaksono, K. S., and Utami, S. R.: Volcanic deposits thickness and distance from mt Semeru crater strongly affected phosphate solubilizing bacteria population and soil organic carbon, J. Ecol. Eng., 24, 360–368, https://doi.org/10.12911/22998993/170860, 2023.

Valeeva, L. R., Dague, A. L., Hall, M. H., Tikhonova, A. E., Sharipova, M. R., Valentovic, M. A., Bogomolnaya, L. M., and Shakirov, E. V.: Antimicrobial activities of secondary metabolites from model mosses, Antibiotics, 11, 1004, https://doi.org/10.3390/antibiotics11081004, 2022.

Valitova, J. N., Sulkarnayeva, A. G., and Minibayeva, F. V.: Plant sterols: Diversity, biosynthesis, and physiological functions, Biochemistry, 81, 819–834, https://doi.org/10.1134/S0006297916080046, 2016.

Vilhelmsson, O., Sigurbjornsdottir, M. A., Thorsteinsdottir, G. V., Cascone, M., Corso, D., Tonietti, L., Migliaccio, F., Nappi, N., Ricciardelli, A., Selci, M., Montemagno, F., Barosa, B., Bastoni, D., Bastianoni, A., Cordone, A., and Giovannelli, D.: Diversity of thermophilic prokaryotes, in: Thermophilic anaerobes. Grand Challenges in Biology and Biotechnology, edited by: Scully, S. M., 21–90, https://doi.org/10.1007/978-3-031-41720-7_2, 2023.

Vilmundardóttir, O. K., Sigurmundsson, F. S., Møller Pedersen, G. B., Belart, J. M. C., Kizel, F., Falco, N., Benediktsson, J. A., and Gísladóttir, G.: Of mosses and men: Plant succession, soil development and soil carbon accretion in the sub-Arctic volcanic landscape of Hekla, Iceland, Prog. Phys. Geogr., 42, 765–791, https://doi.org/10.1177/0309133318798754, 2018.

Vogts, A., Moossen, H., Rommerskirchen, F., and Rullkötter, J.: Distribution patterns and stable carbon isotopic composition of alkanes and alkan-1-ols from plant waxes of African rain forest and savanna C3 species, Org. Geochem., 40, 1037–1054, https://doi.org/10.1016/j.orggeochem.2009.07.011, 2009.

Volk, M., Bassin, S., Lehmann, M. F., Johnson, M. G., and Andersen, C. P.: 13C isotopic signature and C concentration of soil density fractions illustrate reduced C allocation to subalpine grassland soil under high atmospheric N deposition, Soil Biol. Biochem., 125, 178–184, https://doi.org/10.1016/j.soilbio.2018.07.014, 2018.

Wakeham, S. G. and Canuel, E. A.: Biogenic polycyclic aromatic hydrocarbons in sediments of the San Joaquin River in California (USA), and current paradigms on their formation, Environ. Sci. Pollut. Res., 23, 10426–10442, https://doi.org/10.1007/s11356-015-5402-x, 2016.

Wang, H., Wang, J., Xiao, M., Ge, T., Gunina, A., and Jones, D. L.: The fate of amino acid and peptide as affected by soil depth and fertilization regime in subtropical paddies, Sci. Total Environ., 889, https://doi.org/10.1016/j.scitotenv.2023.164245, 2023.

Wijesinghe, J. N., Koarashi, J., Atarashi-Andoh, M., Saito-Kokubu, Y., Yamaguchi, N., Sase, T., Hosono, M., Inoue, Y., Mori, Y., and Hiradate, S.: Formation and mobility of soil organic carbon in a buried humic horizon of a volcanic ash soil, Geoderma, 374, https://doi.org/10.1016/j.geoderma.2020.114417, 2020.

Wygel, C. M., Peters, S. C., McDermott, J. M., and Sahagian, D. L.: Bubbles and Dust: Experimental results of dissolution rates of metal salts and glasses from volcanic ash deposits in terms of surface area, chemistry, and human health impacts, Geohealth, 3, 338–355, https://doi.org/10.1029/2018GH000181, 2019.

Yakimov, M. M., Lünsdorf, H., and Golyshin, P. N.: *Thermoleophilum album* and *Thermoleophilum minutum* are culturable representations of group 2 of the Rubrobacteridae (Actinobacteria), Int. J. Syst. Evol. Microbiol., 53, 377–380, https://doi.org/10.1099/ijs.0.02425-0, 2003.

Yang, Y. R., Guo, Y. X., Wang, Q. Y., Hu, B. Y., Tian, S. Y., Yang, Q. Z., Cheng, Z. A., Chen, Q. J., and Zhang, G. Q.: Impacts of composting duration on physicochemical properties and microbial communities during short-term composting for the substrate for oyster mushrooms, Sci. Total Environ., 847, https://doi.org/10.1016/j.scitotenv.2022.157673, 2022.

Yokobe, T., Hyodo, F., and Tokuchi, N.: Volcanic deposits affect soil nitrogen dynamics and fungal–bacterial dominance in temperate forests, Soil Biol. Biochem., 150, https://doi.org/10.1016/j.soilbio.2020.108011, 2020.

Yucel, T. B.: Chemical composition and antimicrobial and antioxidant activities of essential oils of *Polytrichum commune* (Hedw.) and *Antitrichia curtipendula* (Hedw.) Brid. grown in Turkey, International Journal of Secondary Metabolite, 8, 272, https://doi.org/10.21448/ijsm.945405, 2021.

Zechmeister, H. G., Richter, A., Smidt, S., Hohenwallner, D., Roder, I., Maringer, S., and Wanek, W.: Total nitrogen content and δ15 N signatures in moss tissue: indicative value for nitrogen deposition patterns and source allocation on a nationwide scale, Environ. Sci. Technol., 42, 8661–8667, https://doi.org/10.1021/es801865d, 2008.

Zeglin, L. H., Wang, B., Waythomas, C., Rainey, F., and Talbot, S. L.: Organic matter quantity and source affects microbial community structure and function following volcanic eruption on Kasatochi Island, Alaska, Environ. Microbiol., 18, 146–158, https://doi.org/10.1111/1462-2920.12924, 2016.

Zhang, J., Cai, L., Yuan, D., and Chen, M.: Distribution and sources of polynuclear aromatic hydrocarbons in Mangrove surficial sediments of Deep Bay, China, Mar. Pollut. Bull., 49, 479–486, https://doi.org/10.1016/j.marpolbul.2004.02.030, 2004.